CHALMERS

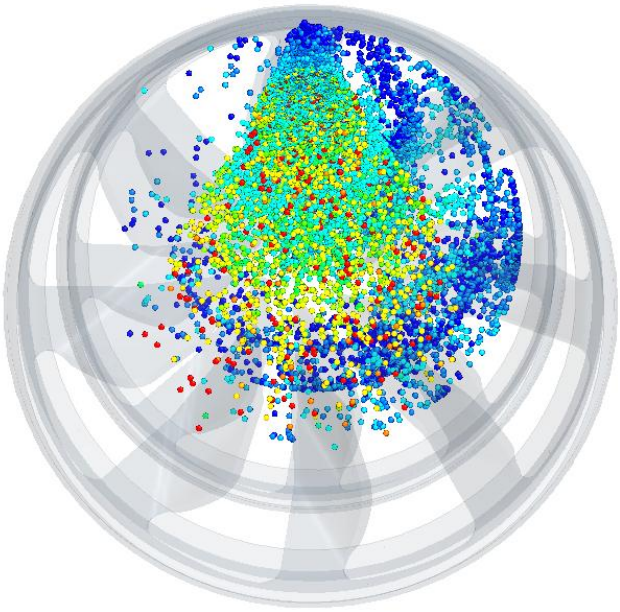

A CFD Study of the Urea Supply, Droplet Breakup and Mixing in a Pipe Upstream of a SCR Catalyst

A design application under development at Volvo Penta

Master´s thesis in the Master´s program Innovative and Sustainable Chemical Engineering

EMELIE SAMUELSSON
SARA HOLMBERG

Department of Chemical and Biochemical Engineering
Division of Chemical Engineering
CHALMERS UNIVERSITY OF TECHNOLOGY
Gothenburg, Sweden, 2013

Cover: The front page shows the urea-water spray and two static mixers from an upstream position.

A CFD Study of the Urea Supply, Droplet Breakup and Mixing in a Pipe Upstream of a SCR Catalyst
A design application under development at Volvo Penta
EMELIE SAMUELSSON
SARA HOLMBERG

Department of Chemical and Biological Engineering
Chalmers University of Technology
SE-412 96 Göteborg
Sweden
Telephone + 46 (0)31-772 100

Preface

This Master of Science thesis has been performed by Emelie Samuelsson and Sara Holmberg, both students at the *Innovative and Sustainable Chemical Engineering* Master's program at Chalmers University of Technology, Gothenburg, Sweden. All work has been equally divided and executed in an equal manner. The work was performed in collaboration with FS Dynamics, Volvo Penta and the Department of Chemical and Biochemical Engineering at Chalmers University of Technology, during the spring 2013. The supervisor of the Master of Science thesis was Dr. Jonas Edman at FS Dynamics and examiner was Assistant Professor Ronnie Andersson at Chalmers University of Technology.

Acknowledgements

First, we would like to thank our supervisor Jonas Edman for all help and support during the project. We would also like to express our gratitude to Sture Wingård and Ulrika Grimfeldt for their enthusiasm and useful input to the project. We would like to thank Assistant Professor Ronnie Andersson and Professor Bengt Andresson for the rewarding discussions regarding difficulties in analyzing our results. We would also like to thank Tony Persson for giving us feedback on the report and all other members in the CFD master thesis group within FS Dynamics for the pleasant meetings and helpful discussions during the project. We would also like to thank everyone at the department at Volvo Penta for an enjoyable environment and for lending us their computers when we needed it most.

Finally, we would like to express our gratitude to our families and friends for their support and love in both rainy and sunny days.

Abstract

The reduction of NO_X emissions from diesel engines by urea SCR (Selective Catalytic Reduction) is a well-established technique. The European standard emission levels are continuously tightened which put high demands on the aftertreatment system. In order to improve the mixing capacity and the breakup of the urea spray in the SCR system, static mixers can be installed. In this thesis a worst case scenario is studied where a pipe based mixing system is used upstream of the SCR resulting in limited time and space for evaporation and mixing. The aim was to study the mixing of the urea spray and the exhaust gas in the mixing pipe by means of CFD simulations. The interaction between the spray, the mixers and the turbulent flow field has been studied. Methods for evaluating the SCR performance through CFD simulations were also improved and developed.

The simulations were performed in STAR-CCM+ v.8.02.008 and the studied geometries were pre-processed in ANSA v.14.0. An engine operating point that has shown low NO_X reduction was used for the simulations. The geometry studied include the mixing pipe upstream of the SCR catalyst which was complemented with one, two or three mixers at different positions in order to determine which configuration that gives the most favorable results. Different injector strategies have also been investigated. In order to capture the behavior of the spray due to the pulsating injector, transient simulations were performed. A sensitivity analysis of the turbulence model, mesh density and inlet velocity profile was performed. The single phase flow was modeled using the Realizable k-ε model and the multiphase flow was modeled using the Euler-Lagrange framework.

Two new measurement methods were developed; *Urea Conversion* and *Stoichiometric Area Index (SAI)*, in order to better estimate the mixing performance and NO_X reduction. It was shown that the urea conversion is strongly dependent on the droplet size and the residence time of the droplets. The *SAI* is dependent on both the urea conversion and the mixing performed by the bulk flow. Further it was concluded that introducing mixers in the system increases both the urea conversion and *SAI* which results in increased NO_X reduction. The highest urea conversion was obtained for the case with three mixers at 50, 100, and 150 mm downstream of the injector. The highest *SAI* was reached when two injectors were used. Since *SAI* reflects the possible NO_X conversion this case was considered to be the most favorable in this study. It has potential to reach an even higher *SAI* if an injector with a lower mass flow is used.

Contents

1 Introduction

1.1 Background

Nitrogen oxides or NO_X is an undesired pollutant in the exhaust gases produced in the combustion process of a diesel engine due to non-ideal conditions [1]. The European emission standards regulates the allowed emission level of NO_X from diesel engines and this level has decreased significantly during the last decade and is supposed to decrease even more in the near future. The non-road diesel engines produced at Volvo Penta contain a SCR system to reduce the amount of NO_X in the exhaust gases. In such system, ammonia (NH_3) is used as a reducing agent to convert NO_X into nitrogen gas (N_2) and water (H_2O) [2]. Since NH_3 is an unhealthy chemical even at low concentrations, urea is used as a NH_3 source [3]. In a urea based SCR system a solution of urea (32,5wt %) and water called AdBlue is injected into the hot exhaust gases through atomization. The water has to evaporate before urea may decompose to NH_3 [4]. Naturally, to obtain a high NO_X conversion over the catalyst, it is of importance to achieve a high conversion of urea and a uniform mixture between NO_X and NH_3. In order to achieve this, static mixers can be installed to enhance the turbulence and break up the spray into smaller droplets.

Computational Fluid Dynamics (CFD) has been an important tool for designing and developing exhaust gas aftertreatment systems in the automotive industry. The process of evaluating the SCR performance experimentally by measuring the NH_3 concentration at the inlet of the SCR catalyst is a difficult task that is both expensive and time consuming. However, numerical methods and computational technologies are developed rapidly which enables CFD simulations to predict the atomization and chemical reactions taking place in an SCR system along with the flow mixing. Hence, by predicting the flow uniformity through CFD simulations the time for the development progression has declined significantly [5].

Volvo Penta produces diesel engines for many different applications with varying space limitations. This means that for some applications there may be sufficient space to obtain both a high conversion of urea and a good mixing of NH_3 and NO_X before the catalyst inlet is reached. However, in some applications the space is very limited, meaning that the mixing system where the injection of AdBlue, decomposition of urea and mixing takes place has to be very compact. Regardless of the application, the amount of released NO_X has to be within the allowed level and preparation has to be done for the future when the allowed level is supposed to be reduced even more.

This study is based on a worst case scenario where the mixing system upstream of the SCR catalyst is a short and straight pipe which is a challenge in terms of urea conversion and flow mixing due to the short residence time. To obtain an enhanced SCR performance the mixing pipe in this study is complemented with static mixers that can create turbulence which favours flow mixing and can interact with the spray by reducing the droplet size. The performance of different designs has been evaluated by predicting the outcome through CFD simulations.

This master thesis is based on a former study at Volvo Penta that analyzed the effect of including one mixer into a mixing-system. How the results changed when the position of the mixer was varied was also investigated in the former study. Based on the earlier gained knowledge this study aims to deepen the understanding of the system and further analyze possible improvements by introducing additional mixers.

1.2 Purpose

The aim of this thesis is to study the mixing phenomena of urea and exhaust gases in the mixing pipe which is located upstream of the SCR catalyst. The interaction between the spray, the turbulent flow field and the mixer elements is studied. The results are assessed as trends in order to get a better knowledge of how the system works and what modifications that will improve the results in terms of urea conversion and the mixing performance. The methods for evaluating the system performance are analyzed and developed in order to get a better estimation of the NO_X conversion.

1.3 Constraints

- Since there are very little experimental data available, the results from the study cannot be validated. A comparison between two turbulence models has been performed in order to analyze the sensitivity on the result between suitable turbulence models.
- The reactions modeled in the study are limited to the urea decomposition in the bulk phase due to both technical and practical limitations.
- To evaluate the NO_X conversion, the mole relation between the involved species over a cross-section at inlet of the SCR catalyst is studied.
- The exhaust gas is simulated as air since the surface chemistry is not modeled.
- The geometry used in the simulations is cut 5 cm into the catalyst in order to make the simulations less computationally expensive.
- The possible modifications of the mixing pipe are physically limited by a flex pipe positioned between the mixing pipe and the SCR inlet. It is not possible to position any mixer inside the flex pipe.
- A simplified geometry of the system was used, where flanges located at the beginning and end of the flex pipe were removed.

2 Diesel combustion and Regulations

2.1 Combustion and emissions

Diesel engines combusts hydrocarbons and the products at ideal conditions are carbon dioxide (CO_2) and water (H_2O). Consequently, the exhaust gas from the engine will primarily consist of CO_2, H_2O and unused air from the combustion. If the conditions are not ideal, pollutants are produced in addition to CO_2 and H_2O. Some of these pollutants have undesirable impact on the environment and/or health. Common pollutants are unburned hydrocarbons (HC), carbon monoxide (CO), nitrogen oxides (NO_X) and particulate matter (PM) [1]. Nitrogen oxide emissions (NO_X) include nitric oxide (NO) and nitrogen dioxide (NO_2).

For non-road diesel engines there are European emission standards to regulate the allowed released emission limit, which are known as Stage $I - IV$. The allowed NO_X level for engines between 130 and 560 kW during the period 1999-2014 is shown in Figure 1. The first legislation for emissions from non-road diesel engines in Europe was implemented in two steps; Stage *I* was introduced in 1999 and Stage *II* from 2001 to 2004 depending on the power output of the engine. The emission limits specified in these two stages were so called engine-out limits meaning the emissions prior to any exhaust aftertreatment device. Stage *III*, which is further divided into Stage *III A* and Stage *III B* was implemented in 2006-2008 and 2011-2013 respectively and the standards in Stage *IV* will be introduced 2014. These standards additionally include an emission limit for ammonia. In Stage *III B* a limit of 0.025 g/kWh of particulate matter were introduced and to reach this limit the use of a particulate filter after the engine was anticipated. The upcoming Stage *IV* has a significantly lower limit of NO_X which likewise is expected to require a NO_X aftertreatment device to be developed [6].

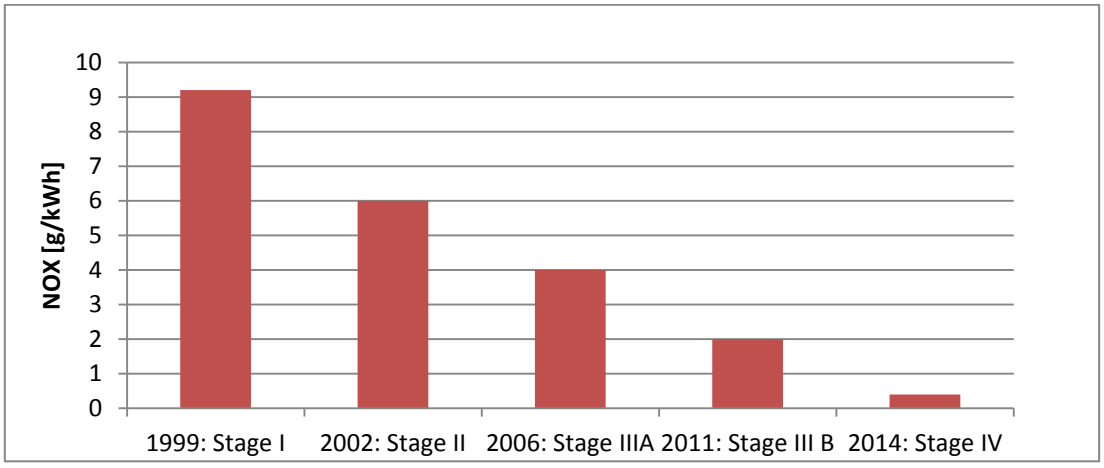

Figure 1: The levels of the European standards Stage I-VI and the year introduced.

2.2 NO_X aftertreatment techniques

In order to meet the upcoming standard levels concerning NO_X discharge, some aftertreatment device is required. There are different technologies for aftertreatment of NO_X and some of the most common techniques available today are:

- *Lean NO_X catalysts* where hydrocarbons are added to the exhaust gases reduce NO_X and forms nitrogen, carbon dioxide and water. The main disadvantage with these types of catalysts is the relatively low NO_X conversion (10-20%). This technology is therefore not seen as a possible technology to meet the future standards [2].

- *NO_X adsorbers* which can be used together with Lean NO_X catalysts and adsorb NO_X at low temperatures where the Lean NO_X catalyst have poor performance. The adsorbed NO_X is then released at temperatures that promote the reaction with hydrocarbons [2]. However, NO_X adsorbers are receptive to sulfur poisoning meaning that the adsorption of sulfur causes irreversible catalyst deactivation. This is the main reason for not using this type of catalyst in diesel engines [3].
- *Plasma-assisted catalyst* where non-thermal plasma is used to generate radicals that can reduce or oxidize the NO molecules [7]. Since oxygen is present in the exhaust gases, the oxidation reaction will be the main reaction and NO may be oxidized to NO_2 and the reduction of NO_X will therefore be low. Since the technology is relatively novel, further research is required for evaluating future use in aftertreatment applications for diesel engines and it is not commercially used at the moment [8].
- *Selective catalytic reduction* (SCR) is used in the Volvo Penta applications and is described in 2.3.

2.3 SCR

In a SCR system, ammonia (NH_3) is used as a reducing agent to convert NO_X into nitrogen gas (N_2) and water (H_2O). The main advantage with this system is the high NO_X conversions (90% or higher). The disadvantages involves the space required for the catalyst, high capital- and operating costs, formation of other emissions (NH_3 slip) and formation of undesirable compounds which may lead to catalyst masking and deactivation. The NH_3 slip can be controlled by installing an oxidation catalyst after the SCR system. Although the SCR system has some drawbacks, the technology has been chosen by the majority of the diesel engine manufactures, due to absence of better options to meet the European standards [2].

2.3.1 SCR types

There are three possible ways to introduce NH_3 to the system; anhydrous NH_3, aqueous NH_3 or an aqueous urea solution that decomposes to NH_3. Ammonia is irritating to skin, eyes and mucous membranes even at low concentrations. The potential risk associated concerning storing and handling the gaseous NH_3 is significant and consequentially it is not commonly used. Hydrous NH_3 has a lower vapor pressure than the anhydrous resulting in decreased consequences in case of an accident. In order to avoid direct handling of both anhydrous and aqueous NH_3, urea is often used as an NH_3 source [3].

2.3.2 Urea decomposition

In a urea SCR system, a urea-water solution often referred to as AdBlue is sprayed into the hot exhaust gases. The AdBlue solution contains 32.5wt % urea and 67.5wt % water. The generation of NH_3 in the SCR system is preceded in three steps as described in reactions (1)-(3). In the first reaction, water is evaporated from the AdBlue droplet and the urea is decomposed to NH_3 and iso-cyanic acid (HNCO) though the termohydrolysis in the second reaction. The state of the urea after the water has evaporated is not fully understood according to Birkhold et al. [4] since some authors report the urea to be in gaseous phase and others that the urea is in solid state.

Evaporation of water from the droplets [4]:

$$(NH_2)2CO(aq) \rightarrow (NH_2)2CO\ (s\ or\ g) + 6.9\ H_2O\ (g) \quad (1)$$

Thermolysis of urea into NH_3 and iso-cyanic acid [4]:

$$(NH_2)2CO\ (s\ or\ g) \rightarrow NH_3\ (g) + HNCO\ (g) \quad (2)$$

HNCO in gas phase is quite stable but can easily be converted to NH_3[4] and carbon dioxide through the hydrolysis reaction if the temperature is sufficiently high (400° C or higher) or on the surface of metal oxides at lower temperatures [9].

Hydrolysis of iso-cyanic acid [4]:

$$HNCO\ (g) + H_2O\ (g) \rightarrow NH_3\ (g) + CO_2\ (g) \quad (3)$$

At favorable conditions, one mole urea will consequentially give two moles of NH_3. Since the urea is the only NH_3 source in the SCR, the decomposition is an important step for the overall performance. Both NH_3 and HNCO will react with NO_X at the catalyst surface (HNCO reacts as described in (3) and then with NO_X) and these two species will hereby be called the *active substance*. It has been proved by Yim et al. [9] that the time required to fully decompose the urea is decreased as temperature is increased and vice versa.

The urea thermolysis and HNCO hydrolysis are modeled assuming reacting species in gas phase and the kinetics are specified according to a study of Yim et al. [9]. The kinetics of the thermal decomposition of urea, reaction (2) and (3), has been investigated suggesting that the thermolysis of urea into the active substance is independent on the presence of a catalyst. In contrast, the reaction rate constant of the hydrolysis is larger in the presence of a catalyst than without indicating that the hydrolysis can be accelerated by a catalyst. The reaction rate constants for the thermolysis of urea, k_1, and hydrolysis of iso-cyanic acid, k_2', in absence of a catalyst are presented by Yim et al. [9] as

$$k_1 = 4.9 \times 10^3 \exp\left(\frac{-2.3\times10^7}{RT}\right)$$

$$k_2' = 2.5 \times 10^5 \exp\left(\frac{-6.22\times10^7}{RT}\right)$$

where the activation energies are given in J mol^{-1} K^{-1} and the pre-exponential factors are given in s^{-1}. The constant k_2' is a product of the reaction rate constant and the concentration of water vapour. The concentration of water is high in the exhaust gas stream and will hences not vary. Further k_2' depends highly on the temperature, resulting in high activation energy and a high temperature is needed to induce the reaction. However, the reaction rate of the hydrolysis is increased on the surface of metal oxides i.e. on the catalyst surface at lower temperatures [9].

2.3.3 SCR surface chemistry

There are four key reactions taking place in the SCR [10]:

$$4NH_3 + 4NO + O_2 \rightarrow 4N_2 + 6H_2O \quad (4)$$

$$4NH_3 + 6NO \rightarrow 5N_2 + 6H_2O \quad (5)$$

$$4NH_3 + 2NO + 2NO_2 \rightarrow 4N_2 + 6H_2O \quad (6)$$

$$4NH_3 + 3NO_2 \rightarrow 3.5N_2 + 6H_2O \quad (7)$$

Due to the fact that usually 90% of the NO_X in diesel exhaust gas is NO, reaction (4) is the main reaction of the SCR. Reaction (5) and (7) are slower than the main reaction. Reaction (6) is on the other hand faster than the main reaction which means that equimolar amount of NO and NO_2 is favorable for a high conversion of NO_X [10]. Due to both technical and practical limitations the surface chemistry is not modeled. However, it is assumed that equation (4) is the most significant reaction and that all formed active substance will react with NO_X and that the NO_X only consist of NO.

2.3.4 SCR catalyst

The reactions described in section 2.3.3 takes place on the catalyst surface at active sites which have a relatively even distribution over the surface. The catalyst used in an SCR system is a monolithic catalyst. A monolith consists of square channels running through the whole catalyst substrate, as shown schematically in Figure 2. Monoliths can be prepared entirely from the specific catalyst material or may include some inert material e.g. metallic or ceramic that act as support material, with a catalytic layer applied on the walls of the channels [11]. Since the catalyst is divided into channels there will not be any significant mixing after the gas flow has entered the catalyst. Hence, it is important to distribute the active substance evenly over the SCR catalyst inlet and thereby making it available in all channels. This emphasizes the importance of reaching a uniform mixture prior to the catalyst inlet.

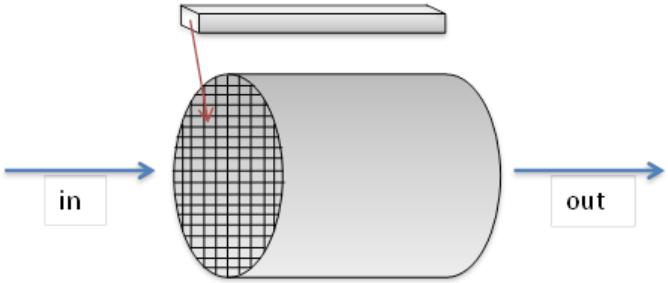

Figure 2: A schematic figure of a monolith catalyst. The substrate is divided into several channels where the reaction takes place on the catalyst surface.

2.3.5 Unwanted reaction paths

At high temperatures, above 400°C, NH_3 may react to nitrous oxide at the catalyst surface and at even higher temperatures the NH_3 may be oxidized, reaction (8) and (9) respectively [12]. Such temperatures are reached at high work load of the engine.

$$4NH_3 + 4NO + 3O_2 \rightarrow 4N_2O + 6H_2O \quad (8)$$

$$4NH_3 + 5O_2 \rightarrow 4NO + 6H_2O \quad (9)$$

Since these reactions consume NH_3, the maximum conversion of NO_X is limited by the amount of reacted NH_3 [10]. The formation of nitrous oxide also contributes to the global warming which is another reason for avoiding this reaction path [12].

During some conditions, uncompleted decomposition of urea can cause formation of undesired high molecular weight by-products which may, at certain conditions, form a solid deposit on the surfaces of the urea SCR system. As a consequence of the incomplete decomposition of urea and formation of deposits, NH_3 formation is also lowered and the catalyst surface may be affected giving a decreased NO_X reduction efficiency. The formation of solid deposits from by-products is mainly dependent on the temperature. In studies made by Xu et. al [13] solid deposits in the SCR has been reported at temperatures below 300°C. At temperatures above 350°C, the majority of the deposits vaporize [13]. Temperatures below 300°C is reached when the engine has a relatively low work load and the exhaust gas stream is not heated to higher temperature.

HNCO plays an important role in many of the routes for by-product formation, both as reactant to form biuret and for further polymerization. A rapid hydrolysis of iso-cyanic acid is favorable since it will decrease the formation of its possible by-products. Examples of undesired by-products are biuret that can react further to cyaunic acid, ammelide, ammeline and melamine [14].

3 Sprays

The AdBlue solution is sprayed into the flow of exhaust gases upstream of the catalyst. The atomization of liquids is a common process unit operation where a bulk fluid is transformed into a spray system. The main intention with atomization processes is to maximize the gas-liquid interface since all transport processes are directly dependent upon this surface area and the exchange between the phases will improve with an increased surface. The exchange between the phases in a spray system increases by several orders of magnitude compared to the case where the liquid is not disintegrated through atomization [15].

3.1 Atomizer

The atomization process itself is the method for breakup of the fluid and produces the resulting spray structure. The principle used is different in different cases and is dependent on the properties of the liquid that is to be atomized. Viscosity, surface tension and density are properties of importance which may vary significantly between different materials. It can be said that the type of the atomizer used in a specific purpose is dependent on:

- The liquid material properties
- The liquid material throughput
- The required spray characteristics

3.1.1 Pressure Atomizer

The atomizer used in most technical applications is the pressure atomizer [15] with a plain-orifice nozzle which is used in the SCR system at Volvo Penta. In a pressure atomizer a pressurized liquid is forced through a small opening (orifice) into a gas at lower pressure and the plain-orifice nozzle produces a full cone spray. The liquid will disintegrate to droplets as a result of the velocity difference. This type of atomizer is typically used for low viscosity liquids [15]. For plane-orifice pressure nozzles the most important feature for the atomization is the dimension of this opening. The finest disintegration is reached when the orifice is small. However, the smaller it is, the more difficult it is to keep the opening free from foreign particles. This means that there has to be a trade-off when choosing the orifice size. Due to this, the minimum size of the orifice is usually limited to approximately 0.3 mm [16]. One drawback with the pressure atomizer is naturally the need of a pressurized liquid but also that the droplets size produced is relatively uneven and the practicable mass flow rate is low [15].

3.2 The simulated injector

The type of injector used in the simulations is a “solid cone” with a spray angle of 42°, i.e. angle b in Figure 3. The principle direction of the spray diverge 50° from a straight injection, i.e. angle a in Figure 3.

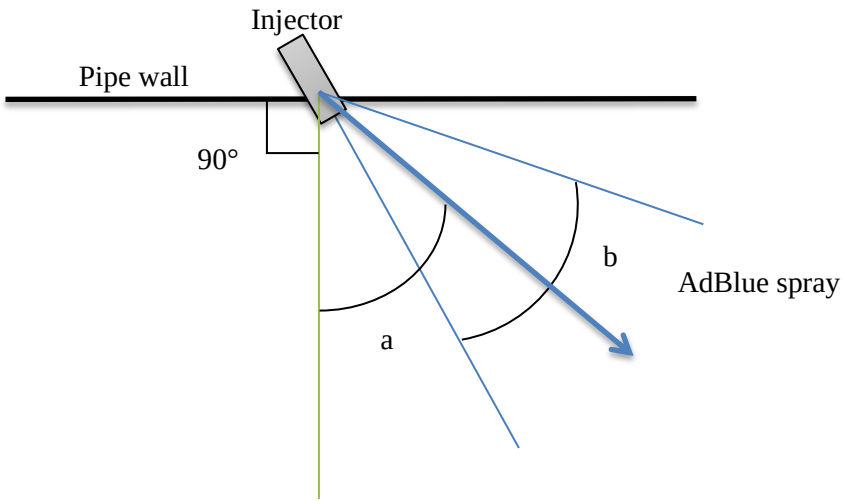

Figure 3: A schematic figure of injector for the AdBlue spray injection. The principle direction of the spray diverge 50° from a straight injection (a=50°) where the straight injection refers to an injection in the normal direction of the mixing pipe wall. The spray angle b is 42°.

In the studied Volvo Penta application, the injector work at a frequency of 4 Hz. This means that urea is injected four times per second at the maximum injection rate of 6.3 kg/h (1.75 g/s). The required mass flow of urea is dependent upon the exhaust gas flow, which varies with the power output of the engine. The total required amount urea per second should then equal the amount injected four times in one second. The time for each injection pulse has to be calculated for each studied power output of the engine. For example if 1 g/s of urea is needed, the injector should inject urea for 0.143 seconds four times when the rate is 1.75 g/s. This type of injection curve is shown in Figure 4.

The injector is simulated as a point where droplets enter the domain with a frequency of 4 Hz and a direction that diverge 50° from a straight injection. The droplet diameters are determined by the Rosin Rammler distribution function described in chapter 3.3. Additionally, the mass flow rate, number of parcels, droplet temperature, mass fractions of the species (urea and water) and the velocity magnitude was specified for the injector.

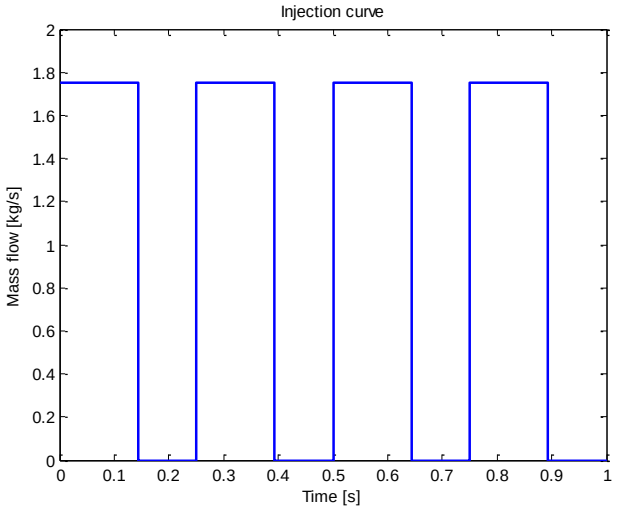

Figure 4: Urea is injected with a frequency of 4 Hz and to get a mass flow of 1 g urea/s the injection time will be 0.143 s. The required amount urea varies with the exhaust gas flow and will be different for each power output.

3.3 Droplet size distribution (Rosin-Rammler)

To describe the droplet sizes of the spray an empirical droplet size distribution function may be used. There are several empirical functions for achieving a droplet size distribution and the choice of function depends significantly on the disintegration mechanism for the situation. One function that has been widely used (and is used in the spray simulations of this study) is the Rosin-Rammler distribution which may be expressed as shown in equation (10).

$$1 - Q = \exp(-\left(\frac{D_p}{X}\right)^q) \tag{10}$$

In this expression, Q represents the portion of the total volume holding drops with a diameter less than D_p. The exponent q is a measure of the spread in size and a higher value means that the spray is more uniform, set to 1.5 in the simulations. X is the reference diameter which in the simulations is set to 93 µm [16].

3.4 Droplet evaporation

There has to be a concentration difference in vapor between the droplet surface and the continuous phase for the evaporation to take place. In most cases the continuous phase surrounding the droplet is assumed to be a binary mixture of the gas and the droplet vapor [17]. The rate of the evaporation process will be determined by the droplet size, temperature, pressure, material properties of the surrounding gas and relative velocity between the phases. One common way to describe steady-state evaporation i.e. when the droplet has reached the wet-bulb temperature that corresponds to the current conditions, is the so called D^2 *law* stated in equation (11) [16].

$$D_0^2 - {D_p}^2 = \lambda t \tag{11}$$

where D_0 is the initial droplet diameter, D_p is the droplet diameter at time t and λ represents the evaporation constant [16]. The evaporation constant may be defined through equation (12).

$$\lambda = \frac{4Sh\rho_c D}{\rho_p}(mf_{A,S} - mf_{A,\infty}) \tag{12}$$

Where Sh is the Sherwood number, ρ_c is an average density for the binary mixture, ρ_p is the density for the dispersed phase (droplets), D is the diffusion coefficient and mf_A is the mass fraction of species A (vapor from the droplets) where s and ∞ indicates at the droplet surface and in the free stream respectively. This means that the evaporation constant will not be constant when the conditions of the surrounding gas changes. However in many applications this may be an acceptable approximation [17].

3.5 Spray-wall interactions

The interaction between the spray and the wall involves complex mechanisms since the outcome of an impinging droplet depends on several parameters including properties of the droplets, the surrounding gas and the wall [4]. Accordingly, there are several different outcomes from an impinging droplet which may be summarized by adhesion, rebound, spread, splash, rebound with break-up and break-up [18]. These possible outcomes and conditions that determine which course of event is the most likely to occur are further discussed in chapter 4.2.1.3.

4 CFD simulations

The simulations have been executed in STAR-CCM+ v.8.02.008. In the following section all models that have been used in the single and multiphase simulations performed in this thesis are described. The theory described in this section is based on the textbook Computational Fluid Dynamics for Engineers [19] and STAR-CCM+ Theory Guide [20].

4.1 Single phase modeling

This section describes the flow characteristics and how these are modeled in the single phase simulations. The single phase flow i.e. the exhaust gas flow and the evaporated NH_3 is modeled as an ideal gas mixture in all simulations of this study.

4.1.1 Modeling the turbulence

A turbulent flow of a fluid can be described as a random and chaotic motion and it is a degenerative process. The large turbulence structures disintegrate into successively smaller structures until the small structures have reached a minimum size and the energy is dissipated into heat. Hence, the turbulence will die relatively quick if no energy is supplied to the system.

Turbulent flows are unsteady in nature, implying that the flow properties are functions of time. To solve the dynamics of such unsteady flows a lot of computational power is required which makes it impractical for industrial applications. Most models therefore solves for mean quantities of the flow. An unsteady flow is therefore in these cases a flow where the statistical mean flow properties vary with time. The turbulent flow in this case can be simulated as steady state since each power output is approximated as steady state, hence the mean properties of the flow does not vary in time. The realizable k-ε model and SST k-ω model, which are described in the following sections, was used to model the turbulent flow and a second order upwind discretization scheme was applied and is further described in section 6.2.1.

4.1.2 Realizable k- ε model

The Realizable k-ε model is a Reynolds Average Navier-Stokes (RANS) model based on the Boussinesq approximation which is described in [19]. It is a two-equation model taking both turbulent velocity and length scale into account. Transport equations are used to describe these variables resulting in that both the turbulence production and dissipation may have different local rates.

In the realizable k-ε model the turbulent kinetic energy, k, is modeled by equation (13) which is a transport equation for k.

$$\underbrace{\frac{\partial k}{\partial t}}_{\mathbf{i}} + \underbrace{\langle U_j \rangle \frac{\partial k}{\partial x_j}}_{\mathbf{ii}} = \underbrace{\nu_T \left[\left(\frac{\partial \langle U_i \rangle}{\partial x_j} + \frac{\partial \langle U_j \rangle}{\partial x_i} \right) \frac{\partial \langle U_i \rangle}{\partial x_j} \right]}_{\mathbf{iii}} - \underbrace{\varepsilon}_{\mathbf{iv}} + \underbrace{\frac{\partial}{\partial x_j} \left[\left(\nu + \frac{\nu_T}{\sigma_k} \right) \frac{\partial k}{\partial x_j} \right]}_{\mathbf{v}} \tag{13}$$

where the different terms describes
i. Accumulation of k
ii. Convection of k by mean velocity
iii. Production of k
iv. Dissipation of k
v. Diffusion of k

To close this equation the energy dissipation rate, ε, and the turbulent viscosity, ν_T, is needed. The dissipation (ε) is modeled with another transport equation and the general form for this is stated in equation (14).

$$\frac{\partial \varepsilon}{\partial t} + \langle U_j \rangle \frac{\partial \varepsilon}{\partial x_j} = \frac{\partial}{\partial x_j}\left[\left(\nu + \frac{\nu_T}{\sigma_\varepsilon}\right)\frac{\partial \varepsilon}{\partial x_j}\right] + C_{\varepsilon 1} S_\varepsilon - C_{\varepsilon 2}\frac{\varepsilon}{k+\sqrt{\nu\varepsilon}} \quad (14)$$

i **ii** **iii** **iv** **v**

where the different terms is describing
i. Accumulation of ε
ii. Convection of ε by mean velocity
iii. Diffusion of ε
iv. Production of ε
v. Dissipation of ε

The turbulent viscosity is then determined through

$$\nu_T = C_\mu \frac{k^2}{\varepsilon} \quad (15)$$

C_μ is a variable determined from an equation. The four closure coefficients in above equations; $C_{\varepsilon 1}$, $C_{\varepsilon 2}$, σ_ε and σ_k are assumed to be constant even though they may vary slightly for different flows.

The realizable k-ε model is valid for most engineering applications. It is advantageous to use since it is relatively robust, economical in terms of computational power and easy to apply. Compared to the standard k-ε model it can handle swirling flows and flow separation because of a modification in the k equation (14) which prevents the normal stresses to become negative. However it is not as stable as the standard k-ε. Another disadvantage is the assumption that the turbulent viscosity is isotropic which means that the convection and diffusion of the Reynolds stresses are not solved.

4.1.3 Two-layer All y+ Wall Treatment

The Realizable k-ε model was used alongside with the two-layer approach which is one method for resolving the viscous sublayer. The computation is split into two layers. In the layer closest to the wall, ε and ν_T is quantified as functions of the distance from the wall. The values of ε that is identified in the near wall region are smoothly blended with the values of ε that is calculated far away from the wall. However the equation for k is solved for the entire flow.

Additionally to the two-layer approach, the all y+ wall treatment in STAR CCM+ was applied. This is a wall treatment that combines the high y+ wall treatment in regions with coarse mesh and the low y+ treatment in regions with fine mesh. In the high y+ wall treatment it is assumed that the cells near the wall lies within the logarithmic section of the boundary layer. The low y+ wall treatment assumes that the viscous sub-layer is accurately resolved and is therefore only valid for turbulence with low Reynolds-numbers. The all y+ treatment also enables realistic solutions for meshes with intermediate resolution i.e. when the cell near the wall lies within buffer region of the boundary layer in the near wall region.

4.1.4 SST k-ω turbulence model

In order to analyze the sensitivity of the solution the SST k-ω turbulence model was used for the simulation. It works well for separating flows and many authors recommend it as the first choice of turbulence model. The model is based on a combination of both k-ε and k-ω models using the first one in the free stream and the latter one in the near wall region. In the original k-ω turbulence model the specific dissipation rate ω is used as a length-determining parameter instead of ε. The equation used to model k is

$$\frac{\partial k}{\partial t} + \langle U_j \rangle \frac{\partial k}{\partial x_j} = \nu_T\left[\left(\frac{\partial \langle U_i \rangle}{\partial x_j} + \frac{\partial \langle U_j \rangle}{\partial x_i}\right)\frac{\partial \langle U_i \rangle}{\partial x_j}\right] - \beta k\omega + \frac{\partial}{\partial x_j}\left[\left(\nu + \frac{\nu_T}{\sigma_k}\right)\frac{\partial k}{\partial x_j}\right] \quad (16)$$

where the different terms describes the same as in the k equation for the k-ε model, equation (13). ω is modeled by

$$\frac{\partial \omega}{\partial t} + \langle U_j \rangle \frac{\partial \omega}{\partial x_j} = \alpha \frac{\omega}{k} v_T \left[\left(\frac{\partial \langle U_i \rangle}{\partial x_j} + \frac{\partial \langle U_j \rangle}{\partial x_i} \right) \frac{\partial \langle U_i \rangle}{\partial x_j} \right] - \beta^* \omega^2 + \frac{\partial}{\partial x_j} \left[\left(v + \frac{v_T}{\sigma_\omega} \right) \frac{\partial \omega}{\partial x_j} \right] \quad (17)$$

and the turbulent viscosity is calculated through

$$v_T = \frac{k}{\omega} \quad (18)$$

The k- ω turbulence model is able to generate better result than the k-ε model in the near wall regions due to the fact that k and ε must go to zero at correct rates at low Re numbers. This is because the dissipation in the equation for ε contains ε^2/k. The All y+ treatment described in 4.1.3 was also used for the SST k-ω turbulence model which is recommended by the STAR-CCM+ theory guide.

4.2 Multiphase modeling

In this section the important parameters in the spray modeling are presented, such as framework for the multiphase simulation and droplet interaction. Since a pulsating injector is used the droplet-phase is modeled transient to solve the pulsating motion of the system. A first order implicit temporal discretization scheme, also called Euler implicit, is applied. Further information about the temporal discretization can be found in section 6.2.1.

4.2.1 The Euler-Lagrange model

In general, the droplets can either be treated as a continuum with the Eulerian approach or tracked individually with the Lagrangian approach. The studied system is defined as a dilute system with a two-way coupling between the phases and these phenomena are described in [19, 21]. This means that the information about the droplets (velocity, size, temperature etc.) travels along the droplet trajectories which are not the case for a continuous phase where information is spread in all directions. The Eulerian approach is therefore not suitable for treating droplets in a dilute flow. Hence, the Lagrangian particle tracking is used for modeling the droplets in the spray [22].

The exhaust gas flow is modeled as a continuum by the realizable k-ε turbulence model with an additional source term that describes the interaction between the continuous phase and the dispersed phase due to the two way-coupling. The AdBlue spray is modeled by tracking the individual droplets i.e. the Eulerian-Lagrangian approach is used for the two-phase flow. The droplets may exchange mass, momentum and energy with the exhaust gas flow. The Lagrangian approach is limited by the number of droplets in the system. Too many droplets will make the simulations too computationally expensive. Naturally, a large number of droplets are needed to represent a typical spray and because of this parcels are tracked instead of individual droplets. A parcel may be defined as a bundle of droplets which all have the same dynamic properties such as velocity and size so that the parcel may be represented by one computational droplet. This means that the local properties of the bundle of droplets can be determined by solving for the properties of the computational droplets as they move through the field [22]. The movement of the parcels is defined as

$$\frac{dx}{dt} = u_p \quad (19)$$

$$m_p \frac{du_{i,p}}{dt} = \sum F_i \quad (20)$$

where equation (19) is the trajectory and equation (20) is the force balance including the relevant forces acting on the parcels. The forces that are commonly included in the force balance are; drag

force, pressure force, virtual mass force, history force, bouyancy force, lift forces, thermophoretic force, brownian force and turbulence force. What forces that should be taken into account in a specific case will be a tradeoff between accuracy of the simulation and required computational power. The studied system is a gas-droplet flow which means that the terms in the force balance that are linearly dependent on the density ratio (gas density/droplet density) may be neglected, since the droplet density is much larger than the gas density. The resulting forces are drag, pressure and buoyancy force. However, the virtual mass force is taken into account in the simulations preformed since including this may enable convergence by making the flow less sensitive to momentum or pressure relaxation factors. The virtual mass force arises when a droplet is accelerated or decelerated and the surrounding fluid is accelerated and decelerated together with the droplet. This means that the droplet seems heavier than it actually is. The simulated spray system does not involve any significant pressure gradient and because of this also the pressure force is neglected. Since the density of the liquid is much larger than the gas density, the buoyancy force of the gas on the droplet will be much smaller than the gravitational force and the buoyancy force is therefore neglected.

Hence, the forces taken into account in the simulations preformed are the drag force and the virtual mass force. The drag force is defined as

$$F_{i,Drag} = \frac{1}{2} A_{proj} C_D \rho_c |u_c - u_p| (u_{i,c} - u_{i,p}) \quad (21)$$

where the drag force coefficient C_D for spherical and rigid droplets, which is assumed in the studied system, are calculated based on the Schiller-Naumann correlation. Further the A_{proj} is the projected area, ρ_c is the density of the continuous phase and u is the velocity denoted by p for the droplets and c for the continuous (gas) phase.

The virtual mass force is defined as

$$F_{i,virt} = -C_{VM} \rho_c V_p \frac{D}{Dt} (u_{i,p} - u_{i,c}) \quad (22)$$

where the virtual mass coefficient, C_{VM}, is set to 0.5 in the performed simulations which means that a volume that is equal to half of the volume of a droplet of the gas phase is accelerated with the droplet. The operator $\frac{D}{Dt}$ denotes the relative acceleration of the droplet in comparison with the continuous phase along the droplet path. V_p represents the volume of the droplet.

4.2.1.1 Turbulent dispersion

When droplet motion is modeled in a turbulent flow the turbulence most often has a significant influence on the droplet motion. The droplets in a turbulent flow are dispersed by the fluctuations of the flow and not by the mean flow. In most cases there is no detailed information describing the turbulence available which means that the turbulent dispersion needs to be modeled. Since the realizable k-ε model is used to simulate the turbulence in this study, only the intermediate-to-large turbulence is modeled and a model is needed to describe the turbulent dispersion. In STAR-CCM+ the turbulent dispersion is modeled by employing a technique called the random walk. The assumption is that the droplets will pass through several eddies in the turbulent flow field and that the droplet remains within one eddy until its lifetime is exceeded. An eddy is defined as a local disturbance in the Reynolds-averaged flow field. The instantaneous velocity, v, that the droplet experience from an eddy is displayed in equation (23) where $\bar{v}$ is the local Reynolds-average velocity of the flow field and v' is the local velocity fluctuations.

$$v = \bar{v} + v' \quad (23)$$

Hence, the term that needs to be modeled is the local velocity fluctuations which is not determined from the RANS model and this is done through

$$v' \approx u_e = \frac{l_t}{\tau_t}\sqrt{\frac{2}{3}} \tag{24}$$

where l_t and τ_t represents the turbulent length-scale and the turbulent time-scale respectively that is gained from RANS based turbulence models.

4.2.1.2 Droplet evaporation

In order to model the evaporation rates of the spray droplets the Multi-Component Droplet Evaporation model is used in STAR-CCM+. The model assumes that the droplets are internally homogeneous and that they consist of an ideally mixed multi-component liquid. The rate of change in mass for each component caused by quasi-steady evaporation is formulated as

$$\dot{m}_{pi} = -\zeta_i g^* A_s \ln(1+B) \tag{25}$$

where B is the Spalding transfer number, A_s is the droplet surface area, g^* is the mass transfer conductance in the limit $B \to 0$ and ζ_i is the fractional mass transfer rate which is defined in equation (26).

$$\sum_T \zeta_i = 1 \tag{26}$$

Here, T is the number of transferred components which may be referred to as the transfer number. It depends on the thermodynamic conditions for the liquid and in practice the number may be positive or negative where the latter one represents condensation. The driving force for the evaporation process is that the system strives towards reaching equilibrium and the state of equilibrium is defined for each component on an ideal vapor-liquid diagram.

4.2.1.3 Bai-Gosman Wall Impingement

When Lagrangian particle tracking is used for modeling the dispersed phase it is also possible to apply the Bai-Gosman Wall Impingement model. This is a method for modeling the droplet impingement and the aim is to predict the outcome after the droplet-wall interaction. There are six possible outcomes which are listed below and also shown schematically in Figure 5.

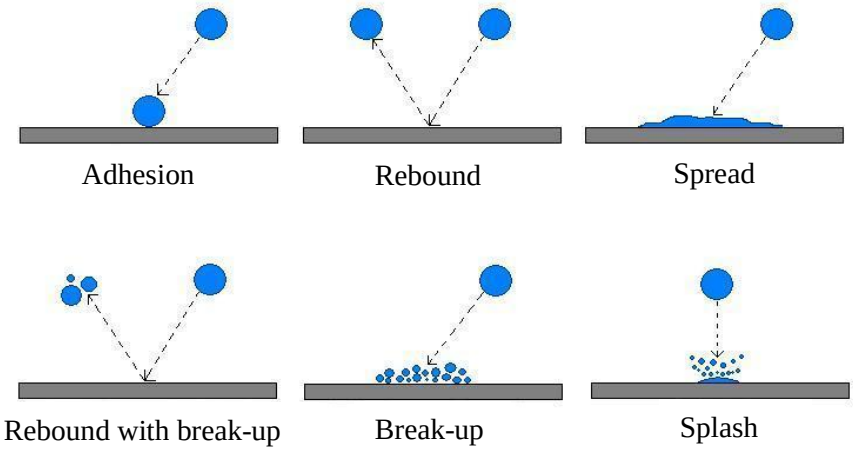

Figure 5: Schematic figure of the possible outcomes for an impinging droplet.

Depending on the occurring regime, one of these six alternatives will be the result of the impingement. The regime is influenced by four parameters; the Weber number, the Laplace number, the wall temperature and the state of the wall. The wall can be either wet or dry. The wall state was set to wet in this study since the spray droplets have a relatively pronounced course and many droplets will impinge the same area. The first droplet that impinges the wall will interact with a dry wall but when many droplets impinge the same area the wall will be wet. Hence to solve the behavior as accurate as possible the state of the wall was set to wet.

The plot presented in Figure 6 displays the different outcome regimes for a wet wall. The defined limits of the axis can be found in the STAR-CCM+ Theory Guide.

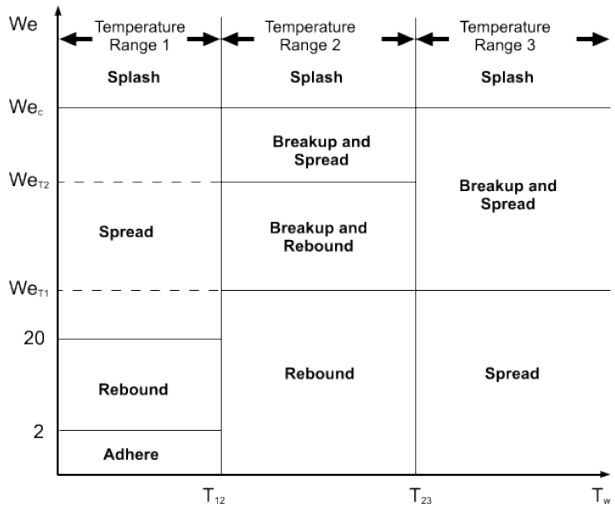

Figure 6: Regime criteria diagram for a wet wall. The Weber number and the temperature will determine the outcome from an impinging droplet for the specific wall state.

5 Important parameters for the SCR performance

The NO_X conversion is affected by the exhaust gas flow field, the mixing capability of the system, supply of the active substance to the catalyst, possible ammonia storage in the catalyst and how the urea is injected among other things. Naturally the NO_X conversion is temperature dependent but this parameter is not varied in this thesis and thereby not discussed here. This section presents these important parameters and how they may affect the SCR performance.

5.1 Effect of the upstream turbocharger

A turbocharger is placed ahead of the SCR system affecting the inlet boundary conditions of the exhaust gas flow. A turbocharger is used to increase the power output of the combustion engine. This is achieved by compressing air before it enters the engine, enabling the engine to work with higher amount of air and fuel input which increases the power output [23]. A turbocharger consists of a centrifugal compressor driven by a turbine which is powered by the exhaust gas from the engine. To get a positive work output from the turbine, the product of the blade speed and the tangential velocity must be larger in the turbine inlet than in the exit. This is often achieved by having a large tangential velocity component at the turbine inlet and allowing little or no swirl of the outlet flow. Depending on the workload of the turbine the exit flow may have different velocities and swirl direction [24]. Experimental data at Volvo Penta has showed an improved NO_X conversion when the turbocharger produce a swirl. The effect of the turbocharger is therefore a parameter that can affect the SCR performance and its effect should therefore be considered in the modeling of the SCR system.

5.2 Mixing

The mixing of AdBlue droplets and exhaust gas is crucial for the SCR performance since a homogeneous mixture is desired to ensure successful evaporation, decomposition and mixing of urea in the exhaust gas. To get an even distribution of the active substance over the catalyst surface, it is also of importance to evenly distribute the urea since active substance will be formed at the positions where urea exists. The mixing process is different depending on the characteristics of the flow, where a turbulent flow gives a more efficient mixing than laminar and is therefore a desired condition. In the following sections the mechanisms for turbulent mixing and the function of a static mixer device are described [25].

5.2.1 Turbulent mixing

A turbulent flow contains random motions over wide scales in terms of length and time which will contribute to the mixing. Mixing on the scale of molecules is driven by molecular diffusion which means that mass is transported due to an existing concentration gradient. Hence, mass is transported from a region with high concentration to a region with a low concentration. The approximate time required for reaching a uniform mixture through molecular diffusion between two fluids with the diffusivity constant D in a domain with the length L may be calculated through equation (27).

$$t = \frac{L^2}{D} \tag{27}$$

Naturally, mixing through molecular diffusion is a very slow process since it takes place on a such small scale [26]. The ability to mix rapidly is one of the main advantageous of turbulence and is referred to as turbulent diffusivity. The random motions on the large scale of turbulence enable mixing and transport of species, momentum and energy much more rapidly than through molecular diffusion [27].

In this study a RANS model is used to describe the turbulence and consequently a turbulent viscosity, v_T, is modeled based on the Boussinesq relation which is described in [19]. It is therefore assumed that the transport of momentum caused by turbulence is a diffusive process and can be modeled by using a turbulent viscosity analogously with molecular viscosity. Furthermore, the turbulent diffusivity D_T may then be calculated as [19]

$$D_T = \frac{v_T}{Sc_T} \tag{28}$$

where Sc_T represents the turbulent Schmidt number which is usually set to 0.7. Hence in analogy with molecular diffusion the length scale, L_T, of the turbulent diffusivity i.e. the length that mass can be transported by the turbulence can be computed through equation (29) [28].

$$L_T = \sqrt{D_T \tau} \tag{29}$$

In this equation τ is the typical residence time in the domain where the mixing is taking place.

5.2.2 Static mixers

One of the big challenges concerning urea SCR systems is to get efficient vaporization of the AdBlue solution and get the produced NH_3 evenly distributed. This could be ensured by design optimization of the mixing domain and the urea injection. However, in some applications there are very strict space constraints and the required length for reaching sufficient mixing and urea evaporation cannot be implemented. In such cases the mixing domain is often complemented with a static mixing device [5]. The mixers are usually positioned after the urea injection and before the catalyst substrate in order to increase the mixing of the system. The introduction of a mixer always increases the pressure drop throughout the system compared to if no mixer is used. Since it is favorable for the mixers to give both low pressure drop and high mixing performance, the design of the mixer is important [29]. The aim of the mixer is to enhance the flow mixing by creating a turbulent flow and to break up the spray into smaller droplets to enhance the evaporation of the AdBlue solution. In this study an eight bladed mixer is used with the blades threaded clockwise in the direction of the flow as can be seen in Figure 7. The position and number of mixers were varied in the simulations in order to determine the most favorable design.

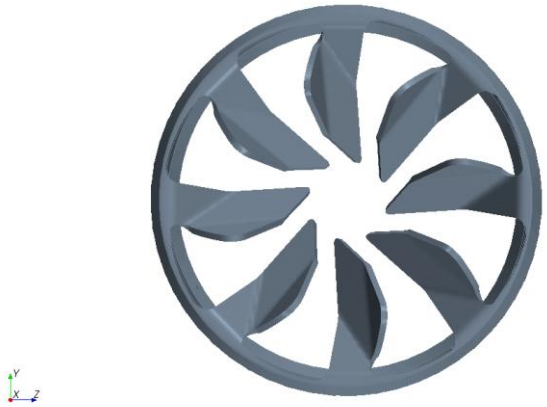

Figure 7: The eight bladed static mixer seen from an upstream position.

5.3 Ammonia storage in the catalyst

In the SCR catalyst NO_X is converted through reaction with NH_3. At certain conditions ammonia may accumulate at the catalyst surface which plays an important role for the performance of the SCR system. Due to the accumulation the actual amount of NH_3 available in the catalyst may differ from the injected amount of NH_3 resulting in excess or deficit of NH_3 giving NH_3 slip or reduced NO_X conversion. The effect of ammonia storage depends on the temperature and at high temperature (above 300°C) there will be limited or no storage capacity. At too low temperatures the adsorption of NH_3 makes no difference since the NO_X conversion is limited by the reaction rate [30].

5.4 Different injection strategies

In the existing Volvo Penta application the spray is injected with a frequency of 4Hz from the pipe wall, as described in chapter 3.2. As mentioned in 0, NH_3 is not stored in the catalyst at high temperatures and the NO_X conversion may therefore be reduced at high engine workloads when a pulsating injector is used. The active substance that reaches the SCR catalyst from one pulse is in excess and should in theory be enough to reduce the NO_X that reaches the catalyst until the next pulse of active substance. However, in practice when the temperature is high and NH_3 is not stored in the catalyst this will not be the case and instead an NH_3 slip is generated along with a reduced NO_X conversion. Hence, when the exhaust gas flow is continuous it is naturally favorable to also have a continuous flow of urea. Additionally the spread of the droplets over the cross section of the pipe is of importance since a more uniform mixture also will increase the NO_X conversion.

Due to this the SCR performance has been evaluated for different injection configurations in order to analyze the effect of the injector type and location of the injector. An injector with a frequency of 4 Hz in the center of the pipe was simulated since it should favor the spreading of the droplets over the cross section of the pipe. A continuous injector is not available at Volvo Penta at the moment; another configuration including two pulsating injectors was studied. The two injectors were placed on opposite sides of the pipe, injecting from the pipe wall with a frequency of 4 Hz but overlapping in time. One of the injectors starts to inject the spray at the start of the simulation and the other one starts to inject when 0.125 s has passed. The AdBlue solution is thereby injected 8 times per second but from two different locations. This should favor the NO_X conversion since the spread of the droplets over the cross section of the pipe should increase. The pulsation of two injectors should ideally cover as large time span as possible in order to reach a more continuous behavior. This could be achieved by using a lower spray mass flow.

6 CFD method

The mixing pipe was simulated in STAR CCM+ v.8.02.008 in 3D and the studied geometry configurations were pre-processed in ANSA v.14.0. This section describes method used in the CDF simulations in this study.

6.1 Geometry

The study focuses on mixing of exhaust gas and urea spray upstream of the SCR substrate and the geometry used for the simulations is therefore only a part of the whole exhaust gas system in order to save computational time. The full-length geometry and the downsized geometry are displayed in

Figure 8 and Figure 9 respectively. The spray injector is located on the same distance from the SCR inlet in all simulations and only the location in y direction has been varied. Additionally the mixer position and the number of mixers have been varied.

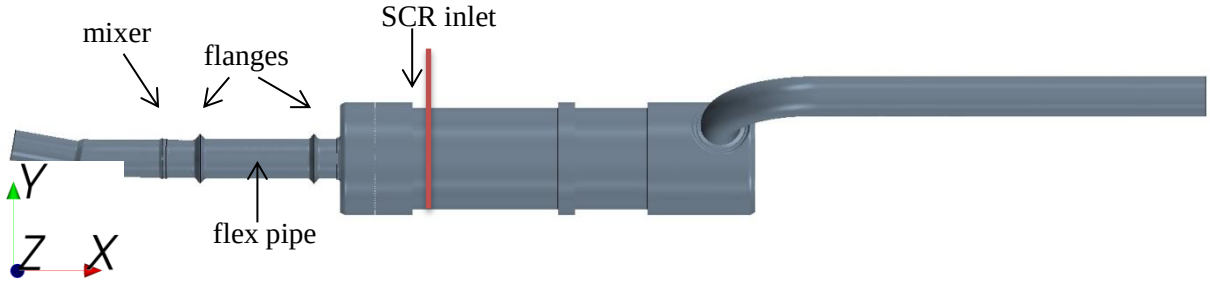

Figure 8: The full-length geometry with one mixer installed and a flex pipe with flanges. This geometry is not used in the simulations where the red line represents a plane where the geometry has been cut off to obtain the downsized geometry.

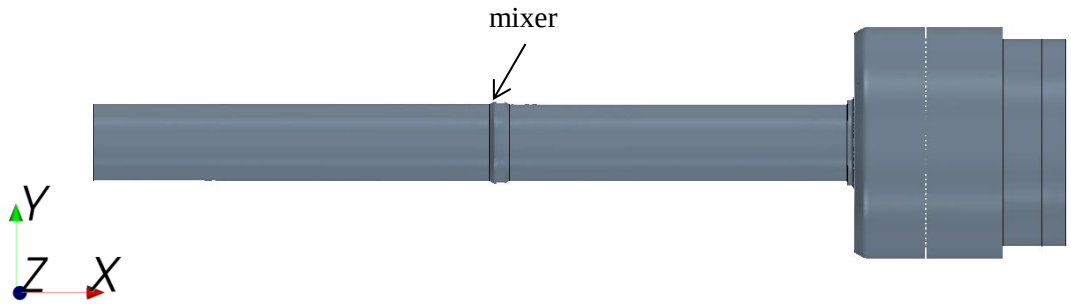

Figure 9: The downsized geometry used in the simulations and in this case with one mixer installed.

To get the correct pressure at the outlet of the studied downsized geometry, a pressure table was exported from steady state simulations for the whole geometry at the specific exhaust gas flow and temperature. Hence, the pressure table was created from a plane inside the full-length geometry that had the location corresponding to the outlet in the downsized geometry. Additionally, the pressure in four points were monitored for the downsized geometry during the simulations and compared to the pressure in the exact same points of the full-length geometry. The difference was used as a convergence criteria which is further described in section 6.3. The exhaust gas flow was simulated at steady state and the spray was added to this flow field as transient simulations.

6.2 Mesh

The volume mesh used in the simulations was a structured mesh aligned with the flow direction and the domain contained 2.2 million cells with a mesh base size of 5 mm. Extrusion was applied to the inlet and outlet boundaries which produced orthogonal extruded cells for these surfaces. This was used

to extend the volume mesh in order to reach a developed velocity profile at the inlet of the real domain. At the outlet the pressure have more time to develop a uniform pressure profile enhancing the convergence. In order to resolve the flow in the near wall region accurately, two prisms layers were used with a thickness of 0.5 mm. The prism layers are important when determining the forces and heat transfer on the walls and flow separation near the wall. Flow separation in turn affects the drag force and the pressure drop which are dependent on the prediction of the velocity and temperature gradients. Due to steeper gradients at the walls the mesh therefore has to be finer. The prism layers also prevent numerical diffusion, which is a result of unphysical transport, and using prism layers therefore gives a more accurate result [20]. The mesh of the geometry with one mixer is shown in Figure 10.

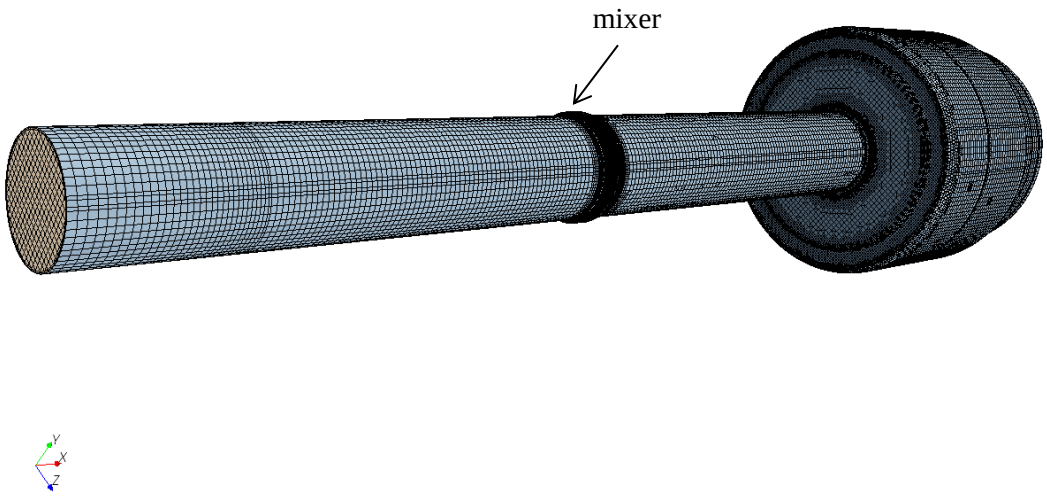

Figure 10: The meshed geometry containing 2.2 million cells with one mixer installed.

The domain close to the mixers was meshed using a denser mesh to properly resolve the gradients in this region. The basic curvature was increased giving a smoother curvature of the mixer, surface size was set to 0.5-1.25 mm affecting the length of the cell sizes and the prism layer. In Figure 11 the mesh refinement applied at the region close to the mixer can be seen.

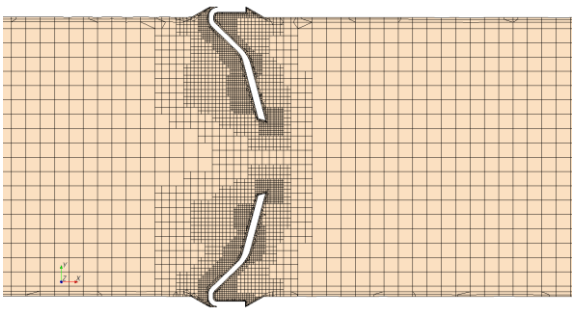

Figure 11: Close up view of the mesh refinement in the region close to the mixer blades.

For the sensitivity analysis the base mesh size was decreased to 4 mm and 3 prism layers were used giving a mesh of 3,4 million cells. The other settings were remained unchanged.

For RANS models it is recommended that y^+ in the near wall region should have a lower limit of approximately 20-30 and an upper limit of typically 80-100 [19]. The y^+ was analyzed in the steady state solutions of the exhaust gas flow and it was found to lie within the recommended limits.

6.2.1 Spatial and temporal discretization schemes

Due to the spatial discretization the cell face values of the grid have to be known to be able to solve the transport equations in every cell. To estimate these spatial discretization schemes are used. In this study the second order upwind scheme is doing this by using information from two upwind cells. Hence, unphysical transport as a result of the discretization is limited giving better accuracy than for a first order upwind scheme [19].

To be able to numerically solve the equations in the transient simulations the time is divided into intervals (time steps). Within each time step sub-iterations are needed to find a solution for that specific time step [19]. A temporal discretization scheme is used to discretize the transient term in the transport equations. In the simulations a first order implicit method, also called Euler implicit was used which uses the solution at the current and previous time level for the discretization [20]. A time step of 0.001 s was used with 10 inner iterations per time step. A maximum of 700 sub-steps for parcel tracking were allowed since it has shown to be a proper time step in previous studies [31].

6.3 Measuring convergence

To measure convergence in the solutions the residuals for continuity, momentum, energy, temperature, turbulent kinetic energy, turbulent dissipation rate and each species were monitored. Further the mass flow in and out of the geometry and the pressure in specific points spread out in the geometry were monitored in the steady state simulations. Convergence was considered to be reached when the values had stabilized.

6.4 Evaluating SCR performance

In order to achieve a high NO_X conversion it is of importance that the system can achieve a high urea conversion. It is also important that the produced active substance is evenly distributed over the SCR catalyst inlet. This section discusses parameters used to evaluate the urea conversion and the mixing performance.

6.4.1 Droplet size and distribution

The amount of produced active substance will depend strongly on the size of the droplets since small droplets will evaporate faster and thereby also react into active substance faster than large droplets. The static mixer(s) that is installed in the system will interact with the spray and break-up droplets into smaller droplets. To investigate this break-up the droplet size distribution in terms of droplet diameter of the droplets passing through a plane downstream the mixer(s) during 0.25 s is studied.

6.4.2 Urea conversion

In order to quantify the performance in terms of active substance production the total urea conversion was calculated. The total mole flow of NH_3 over a plane section inside the SCR catalyst (2 cm from the inlet) during a physical time of 0.5 s was calculated. The mole flow was then integrated, giving a single value of the total mole flow through the plane during 0.5 s. The conversion of urea was then calculated through

$$urea\ conversion = \frac{Total\ mole\ flow\ of\ ammonia}{Total\ mole\ flow\ of\ urea} * 100 \qquad (30)$$

where the total mole flow of urea represents the total moles of urea injected during 0.5 s. Under the assumption that no hydrolysis of HNCO occurs before entering the SCR catalyst, all urea is ideally converted to active substance giving a urea conversion of 100%.

6.4.3 Turbulent length scale

In order to investigate the system capacity to mix the gases through turbulence a turbulent length scale described in 5.2.1 and equation (29) was calculated in a plane cutting through the geometry. An approximate residence time was estimated from the mean velocity and the length of the pipe from the injector. The larger this length scale is the longer distance the turbulence is able to spread the gas inside the pipe. However, note that it is only the gas that is spread by this length scale or more correctly by the turbulent diffusivity. The droplets are spread through turbulent dispersion in the simulations which is described in 4.2.1.1.

6.4.4 Uniformity Index (UI)

To evaluate the mixing performance of the system a uniformity index, UI, can be calculated over the SCR catalyst inlet. The UI compares the local value of a specified scalar to the mean value over the actual surface and is defined as [20]

$$UI\ of\ \emptyset = 1 - \frac{\sum|\emptyset_f - \overline{\emptyset}|A_f}{2|\overline{\emptyset}|\sum A_f} \tag{31}$$

where $\emptyset_f$ is the face value of the arbitrary scalar, $\overline{\emptyset}$ is the mean and A_f the area of the face. A perfectly even distribution generates a value of 1. This index has been used in earlier CFD studies at Volvo Penta for evaluating mixing performance.

6.4.5 Difference in mole relation and Stoichiometric Area Index (SAI)

In order to achieve high conversion over the catalyst it is important that both NO_X and active substance is available in each monolithic channel. The reduction reaction is assumed to be equimolar. In order to ensure high NO_X conversion urea is injected in excess of 10% from the stoichiometric relation. Hence, if all urea is converted to active substance and a completely even distribution is reached for both NO_X and the active substance at the catalyst inlet, the mole relation will be 1:1.1 (NO_X:active substance). Additionally, since the injector is pulsating (with a frequency of 4 Hz) the amount of active substance will be in even more excess at the instant that these species reach the catalyst, see section 3.2 for a more detailed description. As mentioned, ideally the mole relation at the SCR inlet should be 1:1.1 in this case, but it was determined that a relation between 1:1 and 1:1.2 is sufficient to reach a well-functioning SCR. It has been shown experimentally at Volvo Penta that when the mole relation exceed 1:1.2 for the global system, the NH_3 slip becomes unacceptable.

All mole relations between 1:1.21 and 1:∞ is considered to generate NH_3 slip and mole relations between 1:0 and 1:0.99 will instead generate NO_X slip which both are undesirable. To highlight the areas on the SCR catalyst inlet within the acceptable mole relation, the mole relations outside of the acceptable span was cut out from the figures. The areas showed in such figures can be summated for the catalyst inlet and divided by the total area. This gives a single value indicating how large fraction of the inlet having a god distribution of NO_X and active substance. The value will from here on be called *Stoichiometric Area Index* or *SAI* and the definition is shown in equation (32). The index has been used to evaluate the distribution over the SCR catalyst inlet and is indirectly a measure of the mixing performance and the NO_X conversion.

$$SAI = \frac{Surface\ area\ within\ acceptable\ mole\ relation}{Total\ surface\ area} * 100 \tag{32}$$

The injector has a frequency of 4 Hz which mean that the *SAI* will vary with time. In order to take these time variations into consideration a mean *SAI* over the times 0.1 s, 0.2 s, 0.3 s, 0.4 s and 0.5 s was calculated for evaluating the overall performance.

6.5 Simulation set-up

6.5.1 Case study

The conditions in the system in terms of exhaust gas flow, temperature, Adblue flow etc. will vary with the power output from the engine. At some engine power outputs it has been proven to be very difficult to reach high NO_X conversion and will represent a worst case scenario. Therefore such power output has been used in this study. The specifications are presented in Table 1.

Table 1: Conditions for the studied operating point

Name	Exhaust gas mass flow (kg/s)	Exhaust gas temperature (°C)	AdBlue mass flow (g/s)
Case 1	0.281	385	0.994

6.5.2 Mixer and injector configurations

In order to investigate how the system works several system designs have been analyzed. First, static mixers were installed in the system and both number and position of these were varied. Secondly, the effect of the injector was analyzed by varying number and position. All studied configurations have been given a name and these are presented in Table 2 together with their definition.

Table 2: The studied mixer and injector configurations.

Name	Number of mixers	Position (0 at injection) [mm]	Modification to: mixer/injector
100mm	1	100	-
100,150mm	2	100, 150	-
bef&aft flex	2	100, 530	-
bef&aft inj	2	-100, 100	-
50,100mm	2	50, 100	-
50,100,150mm	3	50, 100, 150	-
100,150mm mirror	2	100, 150	Mixer at 150 mm has reversed mixer blades
100,150mm mid inj	2	100, 150	Injection is located in the center of the pipe
100,150mm two inj	2	100, 150	Two 4 Hz injectors injecting half amount each of the required urea, overlapping in time

6.5.3 Boundaries

6.5.3.1 Inlet

The inlet was specified as a mass flow rate inlet where the exhaust gas mass flow and temperature shown in Table 1, was specified. The exhaust gas was modeled as air using mole fractions of 21% oxygen and 79% nitrogen.

Additional boundary conditions are turbulent intensity and turbulent length scale. These were set to 10% and 10% of the pipe diameter respectively since these values have been used in earlier studies at Volvo Penta [31]. To get an estimation of how far into the system these settings will survive, the ratio k/ε multiplied by the average velocity at the inlet was calculated. This gave an estimated survival distance of 0.48 m which is approximately the distance from the inlet to the spray injector. Ideally the turbulent boundary conditions should dissipate before the spray is injected to be sure that there is no effect on the spray droplets. Since correct turbulent boundary condition for the inlet are unknown and since this study is focusing on investigate trends in the system rather than exact values the applied

boundary conditions was used in the simulations of this study. For future simulations when more exact values are of interest it may be required to model the upstream engine device(s) to predict the turbulence at the inlet more correctly.

6.5.3.2 Turbocharger

To investigate how the upstream turbocharger may influence the exhaust gas flow a rotational motion was set as an inlet condition. The swirling flow was assumed to have a direction of ±20° to the main flow direction from which a rotation speed could be calculated. The calculations can be seen in Appendix A.

6.5.3.3 Outlet

The outlet was set to a pressure outlet with a pressure table was extracted from a plane in the full scale geometry at the position of the outlet for the downsized geometry.

6.5.3.4 Wall

The pipe walls were specified as adiabatic and the local pipe wall temperature were set to the temperature of the exhaust gas flow. The walls were also specified with the no-slip condition.

7 Sensitivity analysis

In this analysis the sensitivity of the simulation results depending on turbulence model, mesh density and the inlet velocity profile has been investigated.

7.1 Realizable k-ε vs. SST turbulence model

The two RANS models was described in section 4.1.2 and 4.1.4 and are two possible turbulence models suitable for this study. Since there is no experimental data available, the two models were applied for the simulation configuration *100mm* (see Table 2) and the results were compared to see how the choice of turbulence model affects the solution. The results in terms of mass fractions, UI etc. were very similar when the two turbulence models were compared. This indicates that the choice of the turbulence model in terms of the realizable k-ε model and the SST model does not seem to affect the final results significantly. Since the realizable k-ε model has been used in earlier studies at Volvo Penta, this was chosen also for this study.

7.2 Analysis of mesh independence

In order to analyze how the mesh influences the simulation results two different mesh densities was investigated containing 2.2 and 3.4 million cells respectively. The mixer configuration *100mm*, which is further described in Table 2, and the realizable k-ε model was chosen for this study. This refinement of the bulk mesh should decrease the possible existing numerical diffusion in the coarser mesh. However, no differences could be seen in the results which indicates that the coarser mesh is sufficient for the study.

To further analyze the mesh independence, a refinement could be done for regions where gradients exist in the geometry. An example of a region where significant concentrations gradient exist, is the region where the spray is injected. However, such sensitivity analysis of the mesh was not performed but it is recommended for future studies.

7.3 Analysis of sensitivity to the upstream turbocharger

Since a turbocharger is installed upstream of the mixing pipe in some installations, the effect of applying a swirl on the inlet boundary condition was investigated. At different power outputs the swirl rotates in different directions and since this was a general investigation, it was assumed that the flow at the different power outputs may diverge ±20° from the axis of the flow direction. Three cases were studied; one with no rotating motion at the inlet and two with a rotating motion corresponding to +20° and -20° respectively.

The results showed that a rotating inlet condition will affect the result and how significant the effect will be is dependent on how the mixers are threaded relative the rotation of the flow. Unfortunately, no measured input data for the turbocharger was available which means that the actual inlet condition of the exhaust gas flow could not be simulated. To be able to do this, a simulation of the turbocharger itself has to be performed to achieve the actual flow conditions at the inlet of the mixing pipe. This was determined to be outside the scope of this study and the effect of the turbocharger has therefore not been taken into account in forthcoming simulations. In future work it is recommended to investigate this effect more thoroughly so that correct inlet boundary conditions can be set for the different power outputs. Experimental data at Volvo Penta has showed an improved NO_X conversion when the turbocharger produce a swirl. This indicates that not taking an inlet swirl into account is a conservative way of evaluating the performance of the system. This study aims to investigate a worst case scenario which should be the case when no swirl is generated by the turbocharger.

8 Results and discussion

During this study many different parameters have been studied and analyzed and the understanding of the system has gradually grown. Some of the parameters have shown to be more relevant and important than others and are the ones presented in the report. In this section the simulation results are presented and discussed. The section is divided into three main parts. The first is presenting a characterization of the system and the parameters being evaluated, all described in section 6.4. The second part is an investigation of different mixer positions and number of mixers whereas the third part investigates the effect of position and number of injectors. The configurations investigated are named after the mixer and injector positions where the position of the injector corresponds to zero. For example in the *100mm* configuration the mixer is positioned 100 mm downstream of the injector.

8.1 Characterization of the system

In order to evaluate the modifications that will improve the SCR performance the system was first analyzed, focusing on finding important parameters that are relevant for describing the performance. Three different cases with zero, one (*100mm*) or two (*100,150mm*) mixers were compared. The configurations *100mm* and *100,150mm* are described in Table 2.

8.1.1 Droplet size and distribution

Introducing mixers into the system is important in terms of breaking up the AdBlue droplets into smaller ones as they hit the mixer blades. Smaller droplets require less time to evaporate which enables a higher amount of active substance to form during the same residence time. The efficiency in breaking up the droplets for a system with zero, one or two mixers was investigated by plotting the distribution of the droplet diameters for the three different configurations over a plane downstream of the injector, as is seen in Figure 12. In the case with no mixer, the plane was located 15 cm after the injector and in the mixer cases the plane was located 5 cm from the mixer(s).

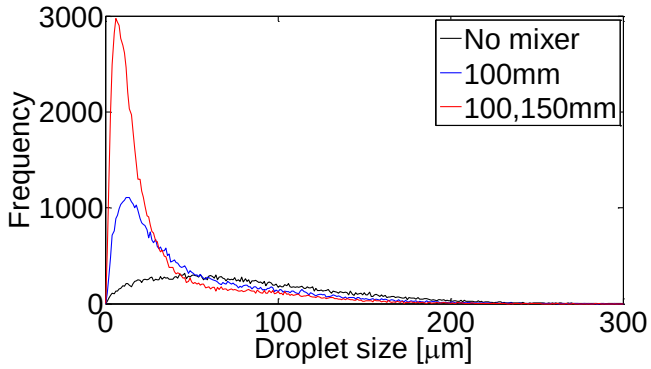

Figure 12: Droplet diameter distribution for a system without, with one or two mixers. The distribution was evaluated in a plane 5 cm downstream of the mixer(s) and 15 cm downstream of the injector in the case without mixer(s).

There are a larger number of small droplets in the system with one and two mixers compared to a system without mixer. This indicates that the mixers efficiently break up the droplets into smaller ones. After the second mixer there are an even higher number of small droplets than after the first mixer which shows that a droplet size equilibrium is not reached after one mixer.

The peak in the droplet diameter distribution is at 6 μm for two mixers and at 12 μm for one mixer which is compared to no mixer that has the peak at 44 μm. This indicates that the second mixer is not as efficient as the first mixer in breaking up the droplets. In order to investigate if equilibrium is

reached after the second mixer in terms of droplet diameter the distribution after a third mixer should be studied.

8.1.2 Urea conversion

The AdBlue droplet size is an important parameter for the active substance formation. In this section urea conversion is analyzed, which is the ratio between the total amount of formed NH_3 and injected urea during a time of 0.5 s. The conversion will be the same for HNCO since the reaction is equimolar and because the hydrolysis HNCO is slow without any catalyst present at the present temperature (385°C). The conversion of urea for the three studied systems is shown in Table 3.

Table 3: Urea conversion for three mixer configurations during 0.5 s.

Configuration	Urea Conversion [%]
No mixer	35
1 mixer (*100mm*)	73
2 mixers (*100,150mm*)	77

The results show the same trend as the distribution of the droplet diameter. The urea conversion increases when mixers are introduced into the system in the same way as the droplet diameter decreases. From a poor conversion of urea in a system without mixer the conversion more than doubles if one mixer is used. The conversion is further increased when a second mixer is introduced. The difference between one and two mixers is not as significant as between none and one mixer, but the conversion increases to some extent. Therefore it is concluded that the urea droplet size has a vital impact on the formation of active substance.

8.1.3 Turbulent length scale

The turbulent length scale was calculated and evaluated in a plane cutting through the system which is displayed in Figure 13. The results show that the case without any mixer has a larger length scale in the middle of the pipe while it is relatively small along the wall (a). The other two systems with one (b) and two mixers (c) instead have larger length scale along the wall and smaller in the middle of the pipe.

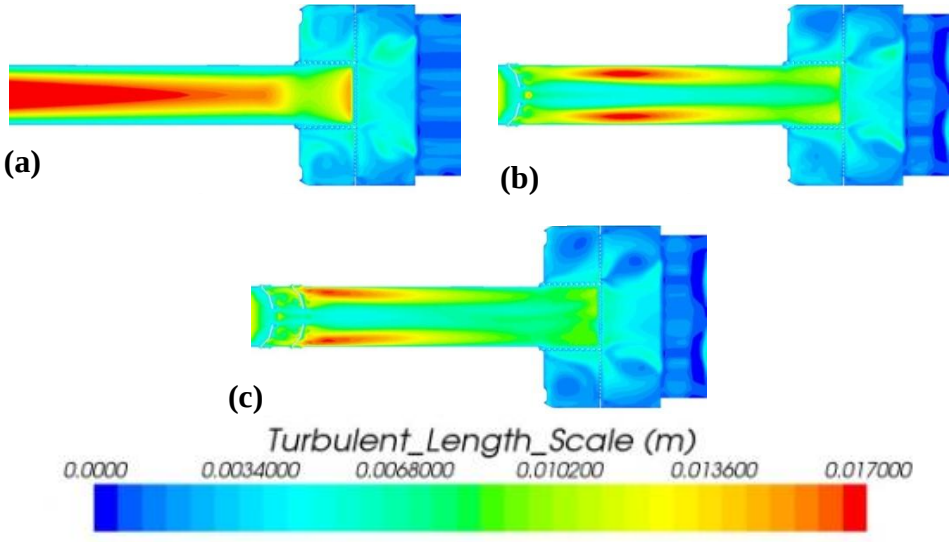

Figure 13: Turbulent length scale for the system without mixer (a), one mixer (b) and two mixers (c) calculated from the turbulent diffusivity and an approximate residence time based on the mean velocity and the pipe length from the injector.

Since the spray is injected from the wall, the small droplets will not penetrate so far in to the pipe but will instead evaporate relatively fast in the area near the wall. On the other hand large droplets are able to penetrate into the middle of the pipe but they will have a much longer evaporation time. This behavior is substantial in the no mixer configuration but not as distinct in the cases including mixers since the mixers enables the droplets to spread. As mentioned earlier, in the modeling turbulent diffusion is only able to transport the gas and will not enhance the spreading of droplets. Hence, a large turbulent length scale along the wall should be favorable which is not the case for the no mixer configuration. However, it is not possible to determine which of the two mixer cases (one mixer and two mixers) that is preferable.

The results also show that the largest length scale is approximately 2 cm and in the systems including mixers it is much lower in the middle of the pipe. Since the pipe diameter is 10 cm the turbulent diffusivity is not able spread and mix the gas over the whole cross section. The droplets will be spread by the bulk flow and a major part of the droplets that evaporates prior to the SCR inlet will evaporate at the end of the domain. This means that the bulk flow has a more important role when it comes to spreading the active substance over the cross section.

The turbulent length scale is received from the steady state solution of the exhaust gases meaning that the spray do not have to be simulated. The reason for this is that the spray in this study is weak and do not produce any significant turbulence itself. On the other hand, when the spray produce turbulence it is not possible to receive the turbulent length scale without simulating the spray. However, in this case the parameter from the steady state solution could be used as an indicator for which system modification that will generate a desirable SCR performance.

8.1.4 Uniformity Index

Earlier studies performed at Volvo Penta applied a surface uniformity index (UI) at the SCR catalyst inlet to evaluate mixing performance of the system. The index was described in section 6.4.3 and compares the face value of a scalar to the mean of the specific scalar and evaluates this for all cells on the surface. A value of one indicates a perfect distribution in terms of UI. This means that a perfect distribution of NH_3 (UI=1) can be achieved even though there are no or very little NH_3 at the surface.

An example of this is given in Figure 14 where UI of the NH_3 mass flux is calculated at the SCR inlet during a physical time period of 0.5 s for the case with no mixer and the case including one mixer. In this figure these two configurations have very similar UI and should therefore have similar distribution of NH_3 mass flux over the SCR inlet. However, the distribution of NH_3 mass flux over the SCR inlet at the physical time 0.4 s (where UI of the two cases are almost identical) in Figure 15 reveals a significant difference between the cases.

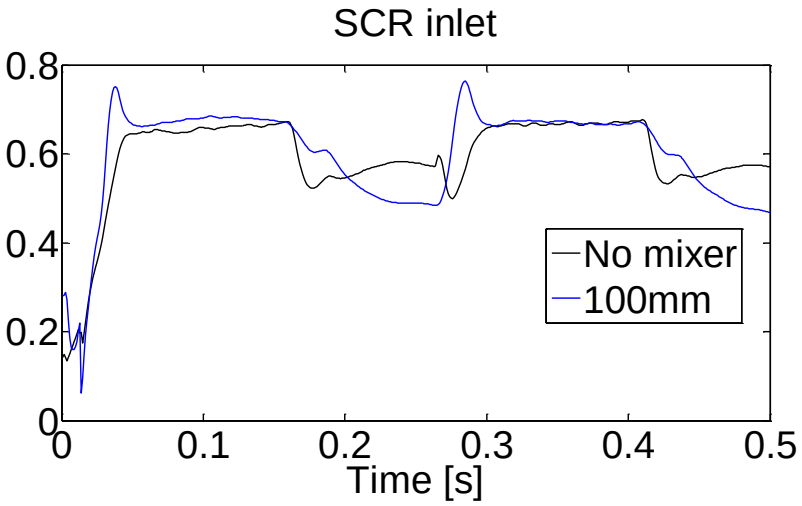

Figure 14: The calculated UI of the mole flux of NH_3 over a physical time period of 0.5 s for the two cases; no mixer and one mixer (*100mm*).

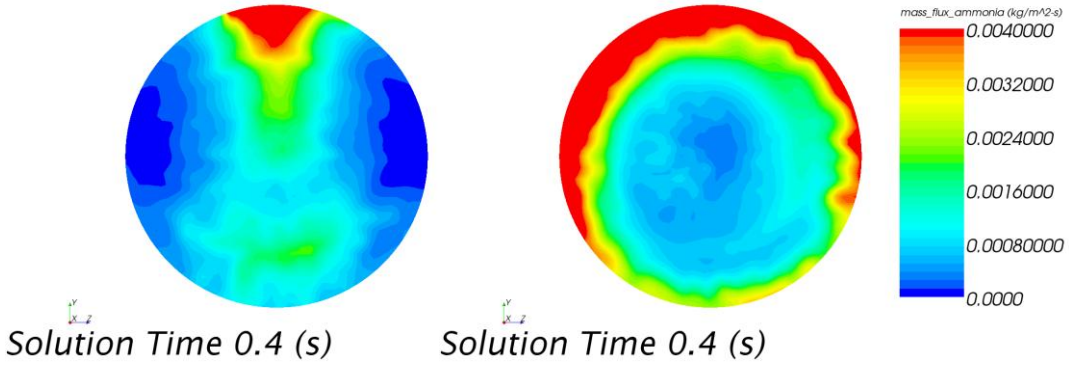

Figure 15: The distribution of NH_3 mass flux over the SCR inlet at the physical time 0.4 s for the two cases; no mixer (a) and one mixer (b).

Figure 15 clearly shows that a system without a mixer (a) do not generate an even distribution of NH_3 while the distribution for a case with one mixer (b) becomes much more even. Nevertheless, the UI for the two cases at this time are almost identical. Since the no mixer case has large areas with very low amount of NH_3 the mean value will be close to zero. It is only a small area at the top of the surface that will diverge from the mean and thereby generating a relatively high UI. Hence, it can be concluded that UI is not suitable for evaluating the current system. Due to this it was decided to exclude UI as a parameter for evaluating the mixing and instead study the difference in mole relation of the involved species at the SCR inlet.

8.1.5 Difference in mole relation and Stoichiometric Area Index (*SAI*)

In order to investigate the NO_X conversion and the mixing performance the area of the SCR inlet having a mole relation between 1:1 and 1:1.2 (as described in 6.4.5) was studied. The result is shown in Figure 16 for the three studied cases. This figure shows that no mixer has the smallest area within the acceptable range which indicates poor mixing performance and the lowest NO_X conversion should be seen in this case. In the system containing one mixer a larger area is reached and it seems to increase even further in the case of two mixers.

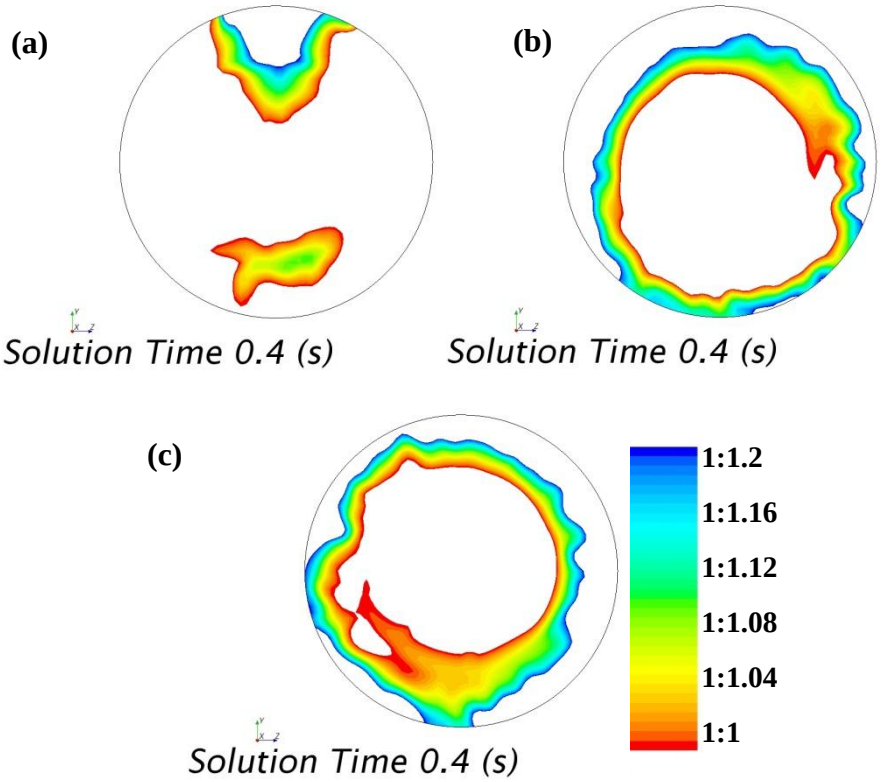

Figure 16: The area that has a mole relation within the acceptable span 1:1 and 1:1.2. The three investigated configurations are no mixer (a), one mixer (b) and two mixers (c).

The *Stoichiometric Area Index* in equation (32) which is also presented in 6.4.5 was calculated in order to quantify the actual area within the specified mole relations for the three system configurations. The results are shown in Table 4. It is confirmed that the area with a mole relation within the specified range, increase with number of mixers. The explanation to this is that the mixers produce turbulence by creating a swirl and thereby changing the velocity profile of the bulk flow. The droplets are spread over the cross-section by means of the bulk flow and the mixing performance is therefore improved when introducing a mixer. Adding a second mixer will change the velocity profile even further and produce an even better mixing. The increase in *SAI* when adding mixers to the system also depends on the decrease in droplet size and the increase in urea conversion. Hence, the system with two mixers produces the largest area with acceptable mole relation at the SCR inlet and it also generated the highest urea conversion. This design should therefore produce the highest NO_X conversion of these three cases.

Table 4: The calculated *SAI* for the three studied system configurations

Configuration	***SAI* [%]**
No mixer	7.2
One mixer (*100mm*)	21
Two mixers (*100,150mm*)	26

The *SAI* value is relatively low for all cases and this is caused by the pulsating injector. The mole flow of active substance will vary considerably with time and will be reduced to almost zero between two injections. To demonstrate the time variations for the reader, a plot of the NH_3 mole flow at the SCR inlet over a physical time period of 0.5 s is shown in Figure 17.

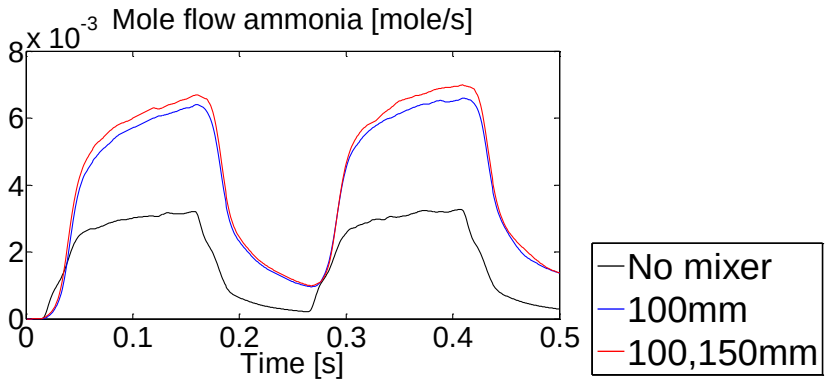

Figure 17: The mole flow of NH_3 at the SCR inlet for the three cases; no mixer, one mixer and two mixers.

The time variations due to the pulsating injector are clearly shown for all three configurations. The two peaks correspond to the two injections taking place in 0.5 s and the mole flow is considerably reduced between the two injections. *SAI* is calculated as a mean value of the area that is reached at the times 0.1 s, 0.2 s, 0.3 s, 0.4 s and 0.5 s which means that the value will be low due to the variations in time. It should be noted that since only five physical times are included in this value it does not take the time variation fully into account. To get a full representation of the variations in time the *SAI* should be calculated over time and then integrated. This is a recommendation for future studies which are further discussed 10.2.

8.1.6 Important parameters for evaluating the SCR performance

In the above result section several parameters have been discussed and their significance for understanding and estimating the SCR performance has been evaluated. It could be concluded that the droplet size will have a strong influence on the urea conversion. Additionally, the urea conversion is a limiting factor for the system and the NO_X conversion is directly connected to this. It can also be concluded that the *SAI* value is an important parameter for evaluating the actual system performance. Hence, these parameters can be used together to evaluate the performance and quantify what system should give the highest NO_X conversion;

1. Droplets size and distribution
2. Urea conversion
3. Stoichiometric Area Index (*SAI*)

In the forthcoming two sections, the SCR performance was evaluated by using these parameters.

8.2 The effect of the positions of two mixers and of introducing a third mixer to the system

The *100,150mm* configuration showed the most favorable results in the previous result section and therefore the effect of the location of the two mixers on SCR performance was investigated. Additionally, the effect of introducing a third mixer to the system was analyzed. Five new configurations were simulated: *50,100mm*; *50,100,150mm*; *bef&aft flex* and *bef&aft inj* and *100,150mm mirror* which are defined in Table 2. All configurations except *100,150mm mirror* have identical mixers installed. In the *100,150mm mirror* case the second mixer (150 mm downstream from the injector) was threaded in the opposite direction compared with the first mixer (100 mm downstream from the injector). The five new configurations were compared to the three cases from the previous section.

The results of the new configurations in terms of urea conversion and *SAI* are presented in Table 5 and these results are analyzed and discussed in the following sections together with the droplet size distribution.

Table 5: The calculated values of the urea conversion and *SAI* for the studied mixer configurations.

Configuration	Urea conversion [%]	Stoichiometric Area Index (*SAI*) [%]
No mixer	35	7.2
100mm	73	21
100,150mm	77	26
50,100mm	78	24
50,100,150mm	80	29
bef&aft flex	74	25
bef&aft inj	79	19
100,150mm mirror	74	28

8.2.1 Urea conversion and droplet size distribution

The urea conversion is presented in Table 5 and the droplet size distribution in Figure 18 for the studied mixer configurations.

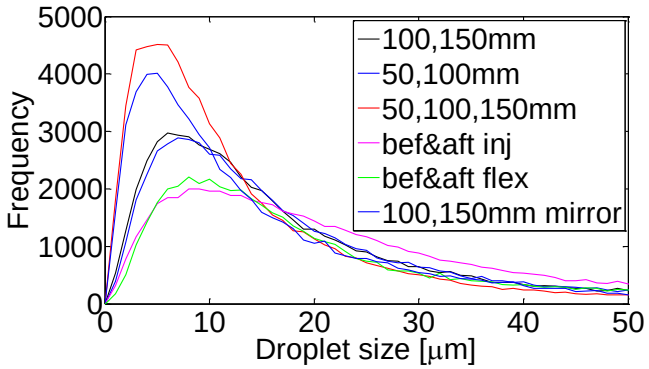

Figure 18: Droplet size distribution for six of the studied mixer configurations.

The urea conversion in the *50,100mm* case is very similar to the *100,150mm* case. The only difference between these cases is that the two mixers are moved 5 cm upstream in *50,100mm* case. This indicates that the mixers are able to break up the droplets similarly in the *50,100mm* case and the *100,150mm* case which is confirmed by the similarities in droplet size distribution. An explanation could be the fact that the spray has a relatively defined direction close to the injection point and only the smallest droplets have started to follow the flow at this position. This could be seen in figures showing the tracked droplets at several points in time meaning that the droplets will impinge at the mixer in similar way.

The case that includes three mixers (*50,100,150mm*) generates the highest urea conversion and further confirms that the urea conversion increases with the number of mixers. Three mixers are able to break up droplets more efficiently than two mixers (*100,150mm*) which can also be seen in Figure 18. However, the increase in urea conversion is smaller between *50,100,150mm* and *100,150mm* than between 10*0,150mm* and *100mm*. The increase in urea conversion when additional mixers are added appears to level out as the number of mixers increase. It seems like equilibrium can be reached by

introducing additional mixers. At such equilibrium the urea conversion cannot be increased further by adding mixers. In order to conclude this, the number of mixers should be increased until no difference can be seen in urea conversion and droplet size distribution and this can be recommended for future studies.

In the *bef&aft flex* case, the conversion is lowered to the level that was also found in the one mixer case (*100mm*). In this system design, both mixers are placed downstream of the injector but only one mixer is located close to the injector. This result indicates that it is important that the droplets interact with mixers and break up early in the system since the mixer at the end of the pipe do not influence the urea conversion. This seems reasonable since if the droplet size is reduced early, the evaporation time will be reduced when the SCR inlet is relatively far away i.e. there is more time for evaporation and conversion of urea. Hence, a larger number of droplets have enough time to evaporate before reaching the inlet of the catalyst.

When one of two mixers was placed upstream of the injector (*bef&aft inj*) a slight increase in urea conversion is seen compared with the *100,150mm* configuration. In this case, the droplets will only interact with one mixer. The difference from the *100mm* case is that one mixer is located upstream of the injector creating a swirl. Consequently the droplets will impinge the mixer differently and the droplet size distribution will be different which is seen from the size distribution in Figure 18. Hence, the droplet breakup is not only dependent on the number of mixers on a close distance downstream. It also depends on the features of the flow field upstream of the injector, which in turn affects how and where the droplets will impinge.

In the last configuration, one of the two mixers were threaded in different direction (*100,150mm mirror*). The urea conversion is in this case similar to the conversion in the one mixer case (*100mm*). However, the droplet size distribution in Figure 18 shows that there are a larger number of small droplets in this case compared to the *100,150mm* case. When the flow is forced to change direction after the first mixer and the fact that the blades of the second mixer has the opposite direction, the efficiency of the second mixer in terms of droplet break up is increased. This confirms the earlier statement, that the droplet breakup is dependent on the features of the flow field upstream of the injector. The reason for the lower urea conversion even though the mixer generates small droplets can be explained by the residence time. It is decreased with 60% compared to residence times for the *100,150mm* case which is seen in Table 11 displayed in Appendix C. The mixers are threaded in different directions which mean that the swirl created from the mixers are canceled out generating a relatively straight flow field and consequently a shorter residence time. This behavior is visualized in Figure 19 where the streamlines for the *100,150mm mirror* case and the *100,150mm* case is compared. This cause a more incomplete evaporation and decreased active substance formation. Hence, the residence time is a second parameter affecting the urea conversion.

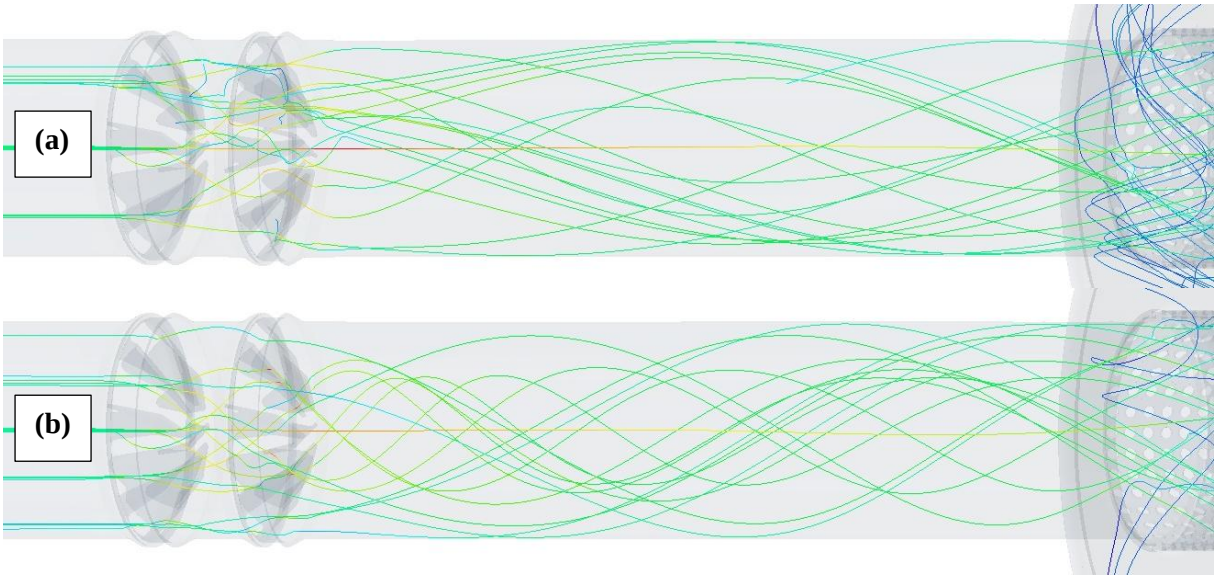

Figure 19: Streamlines visualizing the effect on the flow field of two mixers threaded in opposite direction (*100,150mm mirror*) shown in (a) in contrast to two mixers threaded in the same direction (*100,150mm*) shown in (b).

8.2.2 Stoichiometric Area Index (*SAI*)

As mentioned, changing the position of the two mixers from *100,150mm* to *50,100mm* generated similar urea conversion but the *SAI* value is decreased with 2%. The mixers create turbulence in terms of a swirl that improves the mixing capacity of the system. However, turbulence is dissipative which means that when the mixers are moved upstream the created turbulence will dissipate earlier in the system. This could be the explanation for the decrease in *SAI*.

When introducing a third mixer (*50,100,150mm*) the *SAI* is increased compared to the two mixer case (*100,150mm*). This confirms the conclusion drawn in the previous section that adding another mixer will change the velocity profile even further and produce an even better mixing. Hence increasing the number of mixers enhances the mixing capacity of the system. However, the mixers also generate a pressure drop in the domain which will naturally increase with number of mixers. This has to be considered when designing the system and a trade-off has to be made since a large number of mixers may generate much better mixing but the pressure drop may be unacceptably large. The pressure drops for all studied configurations is presented in Appendix C.

The *bef&aft flex* case generates a lower *SAI* than the *100,150mm* case which indicates that it is more favorable to place the mixers close to the injector than further downstream in the pipe. Hence, it is important to enhance the bulk flow mixing early in the system to reach a more uniform mixture at the inlet.

When one mixer is placed upstream of the injector (*bef&aft inj*) the *SAI* is significantly decreased when compared to the *100,150mm* case. This emphasize the discussion in the *50,100mm* case, that moving the mixers upstream also means that the created swirl from the mixers will dissipate or decrease further upstream in the system.

In the last configuration, one of the mixers were threaded in opposite direction (*100,150mm mirror*) which resulted in a *SAI* almost as high as for three mixers. In all other cases a more unified swirl direction is produced since the mixers have the same mixer blade direction whereas in the *100,150mm mirror* case the flow is forced to change direction after the first mixer meaning that the flow will be divided into several flow directions. This increases the mixing capacity of the two mixers which

results in a higher *SAI* than for the other cases with two mixers. Hence, if two mixers are to be used it is favorable to thread them in opposite directions. The pressure drop over the mixers in the *100,150mm* configuration is the same as the pressure drop for three mixers (*50,100,150mm*) but it is advantageous to use as few mixers as possible in the practical solution. The pressure drops for the configurations are is presented in Table 12 in Appendix C.

8.3 The effect of injector position, number and injection type

There are different ways in which the AdBlue can be injected. In order to investigate the differences between different injector scenarios two different injector strategies were studied using the *100,150mm* configuration; inject the AdBlue in the middle of the pipe and use two injectors injecting one at the time. When the spray is injected in the middle of the pipe, the spray is more evenly distributed over the cross-sectional area which should represent a best case scenario in terms of mixing. A continuous spray should be the best case scenario in terms of feeding the catalyst with reducing agent evenly over time. This continuous behavior is imitated by using two injectors that inject one at the time i.e. the first injector starts to inject at the start of the simulation and the second starts at 0.125 s. In practice this means that active substance will be fed to the catalyst eight times per second instead of four. However, the injection time for each pulse will be shorter. In this section the two injection strategies are studied in comparison to the present injector (*100,150mm*) and the results are evaluated in terms of urea conversion and *SAI*, which is shown in Table 6.

Table 6: The calculated values of the urea conversion and *SAI* for three different injection strategies.

Configuration	Urea conversion [%]	*SAI* [%]
100,150mm	77	26
100,150mm mid inj	61	27
100, 150mm two inj	74	30

8.3.1 Urea conversion and droplet size distribution

The urea conversion is presented in Table 6 and the droplet size distribution in Figure 20 for the studied injector configurations.

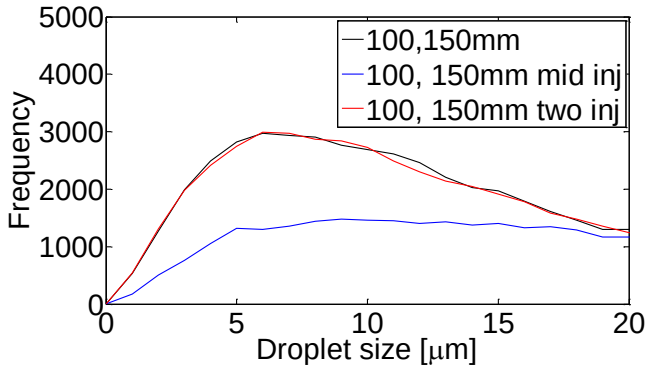

Figure 20: Droplet size distribution for the studied injector configurations.

As seen inTable 6 the conversion of urea is decreased when the spray is injected in the center of the pipe compared to a side injection and this may have several reasons. When the spray is injected in the center of the pipe, a major part of the spray will follow the flow in the middle where the velocity is high and the flow field straight and will therefore have less time to form active substance. This is confirmed by looking at the residence time for the *100,150mm mid inj* in contrast to the *100,150mm*

case in Table 11 presented in Appendix C. Another aspect is the interaction between the droplets and the mixer blades. Since a large number of droplets go straight through the pipe center they will be less affected by the mixer blades and will therefore not break up to the same extent as in the case of a side injection which is seen in Figure 20.

For the case with two injectors (*100,150mm two inj)* the urea conversion is lower than for the case with one side injector (*100,150mm*). Each injector injects the same AdBlue mass flow as one injector but the time duration for each pulse is shorter and the second injector is shifted in time. The injectors are placed opposite to each other and the spray is therefore injected from two directions. As seen from Figure 20 the *100,150mm two inj* generates the same droplet distribution as *100,150mm*. Since the mixers are symmetrical and since the two injectors are positioned symmetric it seems reasonable that the droplet size distribution is similar. The flow field used for the two simulations is also the same but the two cases still have different urea conversion. It can be explained by the time shift in the second injector giving half of the injected AdBlue shorter time to form active substance at the time of evaluating the results. The urea conversion is evaluated over a time period of 0.5 and the residence time over 0.25 s. When a single injector is used almost all droplets from an injection have passed the SCR catalyst inlet in 0.25 s. When two injectors are used there are still droplets left in the system after 0.25 s and 0.5 s resulting in an underestimation of the residence time and the urea conversion. A better way to be able to compare the two cases has to be determined in order to evaluate this specific case but also future cases regarding new injection strategies.

8.3.2 Stoichiometric Area Index (SAI)

As seen from Table 6 the middle injection (*100,150mm mid inj*) increases the *SAI* compared to a side injection. The increase is not as high as expected since the short residence time gives a lower *SAI* between pulses which decreases the time averaged *SAI*.

The two injector case (*100,150mm two inj*) shows the highest *SAI* of all tested configuration. Since the injectors are located opposite to each other the spreading of the droplets are enhanced resulting in a more even distribution at the SCR inlet and a higher *SAI*. Furthermore, injecting the spray alternatingly means that the catalyst is fed with active substance more evenly over time resulting in a higher *SAI* over time. The effect of using two injectors would be even more substantial if a lower mass flow is injected since the pulse duration needed to reach the same average mass flow is increased. The two injector configuration (*100,150mm two inj*) is therefore recommended to investigate further to reach a more continuous feed of active substance to the catalyst. For example an injector with a mass flow of 3 kg/s instead of 6.3 kg/s could be studied.

9 Conclusions

- The *Uniformity Index* (*UI*) is not suitable for evaluating the SCR performance in a system were the amount of produced active substance may be low. It is more relevant to study the actual mole relation between the reactants.

- Two assessment methods have been developed in order to evaluate the performance of the SCR; Urea conversion and *Stoichiometric Area Index* (*SAI*). These were used to evaluate the active substance formation and the mixing performance in the system. It has been shown that the urea conversion is strongly dependent on the AdBlue droplet size and the residence time. Furthermore, *SAI* is dependent on both the urea conversion and the mixing performed by the bulk flow.

- It was concluded that introducing mixers into the system increases both the urea conversion and *SAI* which should result in higher NO_X reduction. The most substantial improvement is seen when one mixer is introduced to the system. Two and three mixers will further improve the performance but the improvement will not be as significant.

- The case with three mixers (*50,100,150mm)* generates the highest urea conversion and it could be concluded that the droplets size is decreased and the urea conversion is increased as the number of mixers are increased.

- The highest *SAI* was reached when two injectors were used (*100,150mm two inj*). Since *SAI* reflects the possible NO_X conversion this case was considered to be the most favorable in this study. It has potential to reach an even higher *SAI* if an injector with a lower mass flow is used.

10 Future studies

10.1 Proposed design for further investigation of the system

It has been shown that *SAI* was radically improved when a second mixer was laterally reversed which indicates that breaking up of the flow is important for the mixing in the system. It is therefore recommended in future studies to find a way to break up the flow but still retain the droplet breakup efficiency to get a high urea conversion. A way to achieve this could be to use another type of mixer for the second mixer position. Hence, the mixer closest to the injector could be the one used in this study which has shown to efficiently break up droplets. The second mixer, located downstream of the first mixer, could have another design that enhances the breakup of the flow.

It could be concluded that the urea conversion increased as the number of mixers was increased. However, it seems like equilibrium exists where the urea conversion cannot be increased further by introducing additional mixers. In order to conclude this, an investigation where the number of mixers is increased until no difference can be seen in urea conversion or specifically in droplet size distribution downstream of the mixers could be performed.

The case that included two injectors was concluded to be the most favorable configuration in this study and this configuration is therefore recommended to investigate further. The position of the mixers, number of mixers and type of mixer could be varied in attempt to find a more optimal design. Additionally, the type of injector can be changed to seek a solution where the catalyst is more evenly fed with active substance. For example an injector with a mass flow of 3 kg/s instead of 6.3 kg/s could be studied.

In this study one operating point has been used for analyzing the performance of different design configurations. Since the performance may be dependent on the workload it is recommended to investigate if the trends for the different configurations in this study also can be seen for other operating points.

In order to increase the accuracy in the simulations it is recommended to include conjugated heat transfer and the liquid film model in future investigations. This would mean that the droplet impingement and the droplet evaporation at the wall can be simulated more correctly giving a more complete description of reality. The flanges on the flex pipe, where it is possible to get accumulation of droplets are also recommended to be included. Further, the effect of the turbocharger could be investigated using outlet data from simulations of the turbocharger at different power operating points.

10.2 Proposed improvement to evaluating methods

One important aspect to further consider in future work is the urea evaporation, if the evaporation is complete or if any droplets remain in the system at the SCR catalyst inlet. It is undesirable that droplets enter the catalyst since it may reduce the NO_X conversion and/or create solid deposits on the catalyst surface depending on the present temperature. In this study indication of an incomplete evaporation has been observed which emphasize the importance of quantifying it. One suggested method is to compare the mole flow of urea in droplet form to the total injected mole flow of urea over the time period of the simulation as displayed in equation (33). Preferably, this could be evaluated over a plane just upstream of the SCR inlet since ideally, all urea is evaporated before entering SCR giving a value of 0%.

$$Urea\ in\ droplet\ form = \frac{Total\ mole\ flow\ of\ urea\ in\ droplet\ form}{Total\ mole\ flow\ of\ urea} * 100 \qquad (33)$$

Another improvement is to take the time dependence into account in the *SAI* used in this study. As already discussed, the spray is pulsating giving significant variations in the mole flow of active substance over time. In this study, *SAI* were evaluated for five times (0.1 s, 0.2 s, 0.3 s, 0.4 s and 0.5 s) and then averaged. However to fully include the time variations the index should be calculated over the time that the simulation is run. The method for calculating *SAI* used in this study is unfortunately not possible to apply for such evaluation and the method has to be further developed. However, if additional times are taken into account in *SAI* the index would represent the time variations to a higher extent and the same routine can be used for this manner.

The principle used to calculate *SAI* can also be used to develop new indexes describing the slip. At a mole relation above 1:1.2 i.e. the active substance is in large excess, the risk of NH_3 slip is substantial. The index for evaluate the NH_3 slip can be calculated in the same way as *SAI* but with a mole relation from 1:1.21 to 1:∞. The same method can be used for determining the NO_X slip, where the mole relation investigated should be between 1:0 and 1:0.99.

11 Bibliography

1. Majewski, W.A. *What are diesel emissions*. 2012 2012-08 [cited 2013 21/2]; DieselNet Technology Guide]. Available from: http://dieselnet.com/tech/emi_intro.php#intro.
2. *Diesel Catalysts*. 2004 2004-05 [cited 2013 21/2]; DieselNet Technology Guide]. Available from: http://dieselnet.com/tech/cat_diesel.php.
3. R. Salib, R.K., *Optimization of Ammonia Source for SCR Applications*, in *2003 Mega Conference*2003.
4. Birkhold, F., et al., *Analysis of the Injection of Urea-Water-Solution for Automotive SCR DeNOx-Systems: Modeling of Two-Phase Flow and Spray/Wall-Interaction*, 2006, SAE International.
5. Zhang, X., M. Romzek, and C. Morgan, *3-D Numerical Study of Mixing Characteristics of NH3 in Front of SCR*, 2006, SAE International.
6. *Nonroad Diesel Engines*. 2010.08 [cited 2013 12/4]; Available from: http://www.dieselnet.com/standards/eu/nonroad.php.
7. *Mechanism of NO reduction with non-thermal plasma.* Journal of Environmental Sciences, 2005. **17**(3): p. 445-447.
8. *Plasma Exhaust Treatment*. 2000 2000-12 [cited 2013 21/2]; DieselNet Technology Guide]. Available from: http://dieselnet.com/tech/plasma.php.
9. Yim, S.D., et al., *Decomposition of Urea into NH3 for the SCR Process.* Industrial & Engineering Chemistry Research, 2004. **43**(16): p. 4856-4863.
10. Koebel, M., M. Elsener, and M. Kleemann, *Urea-SCR: a promising technique to reduce NOx emissions from automotive diesel engines.* Catalysis Today, 2000. **59**(3–4): p. 335-345.
11. Roberts, G.W., *Chemical Reactions and Chemical Reactors*2009: John Wiley & Sons, Inc.
12. Warell, H.R.J., *dikväveoxid*, in *Nationalencyklopedin*2013.
13. Xu, L., et al., *Laboratory and Engine Study of Urea-Related Deposits in Diesel Urea-SCR After-Treatment Systems*, 2007, SAE International.
14. Andreas, L., *Urea Decomposition for Urea-SCR Applications, Experimental and computational fluid dynamics studies*, PhD thesis, *Department of Chemical and Biological Engineering, Division of Chemical Engineering*2010, Chalmers University of Technology: Gothenburg. p. 52.
15. Udo, F., *Spray Systems*, in *Multiphase Flow Handbook*2005, CRC Press. p. 8-1-8-100.
16. Lefebvre, A.H., *Atomization and Sprays*. Combustion: An International Series, ed. N. Chigier1989, United States of America: Hemisphere Publishing Corporation.
17. Crowe, C.T., *Particle-Fluid Interaction*, in *Multiphase Flows with Droplets and Particles, Second Edition*2011, CRC Press. p. 57-117.
18. Chen, C., et al., *Detailed Modeling of Liquid Fuel Sprays in One-Dimensional Gas Flow Simulation*, 2004, SAE International.
19. Andersson, B., Andersson, R., Håkansson, L., Mortensen, M., Sudiyo, R. and van Wachem, B., *Computational Fluid Dynamics for Engineers,* Cambridge University Press, 2012.
20. *STAR CCM+ v.8.02.008 Theory Guide*, 2013.
21. Crowe, C.T., *Properties of Dispersed Phase Flows*, in *Multiphase Flows with Droplets and Particles, Second Edition*2011, CRC Press. p. 17-38.
22. Crowe, C.T., *Droplet-Particle Cloud Equations*, in *Multiphase Flows with Droplets and Particles, Second Edition*2011, CRC Press. p. 235-258.
23. *turboaggregat*, in *Nationalencyklopedin*.
24. Hall, S.L.D.C.A., *Fluid Mechanics and Thermodynamics of Turbomachinery*. 6th ed2010, Oxford: Butterworth-Heinmann.
25. Coulson, J.M., et al., *Coulson and Richardson's Chemical Engineering Volume 1 - Fluid Flow, Heat Transfer and Mass Transfer (6th Edition)*, Elsevier.
26. Webster, P.J.W.R.a.D.R., *Turbulent Diffusion*, in *Environmental Fluid Mechanics: Theories and Applications*2002, American Society of Civil Engineers. p. 7-45.

27. Bourne, J.B.a.J.R., *Turbulent Mixing and Chemical Reactions*1999, Chichester, England: John Wiley & Sons Ltd.
28. Andersson, B., Private communication, 2013.
29. Rajadurai, S., *Improved NOx Reduction Using Wiremesh Thermolysis Mixer in Urea SCR System*, 2008, SAE International.
30. Tsinoglou, D. and G. Koltsakis, *Modelling of the selective catalytic NOx reduction in diesel exhaust including ammonia storage.* Proceedings of the Institution of Mechanical Engineers, Part D: Journal of Automobile Engineering, 2007. **221**(1): p. 117-133.
31. Edman, J., *A urea spray simulation study of a Volvo Penta C15 muffler and the R22 system*, 2012.
32. Tae Joong Wang, S.W.B., and Seung Yeol Lee, *Experimental Investigation on Evaporation of Urea-Water-Solution Droplet for SCR Applications.* AIChE, 2009. **55**(12): p. 3267-3276.
33. Hellsten, S.-E.M.a.G., *DATA OCH DIAGRAM*. 7th ed2008, Stockholm: Liber AB.
34. Efstathios, M. and C. Clayton, *Basic Concepts and Definitions*, in *Multiphase Flow Handbook*2005, CRC Press. p. 1-1-1-79.

A Appendix – Calculation of rpm for the swirling flow

Velocity is equal to the volume flow rate divided by the cross section area of the pipe.

$$v = \frac{q}{A} = \frac{m^3/s}{m^2}$$

To get velocity from a mass flow the density is needed

$$v = \frac{m}{\rho} * \frac{1}{A}$$

Following figure illustrates the velocity component for a 20° deviation from the flow direction. v_x is the velocity in the flow direction and v_s represents the velocity component for a 20° deviation.

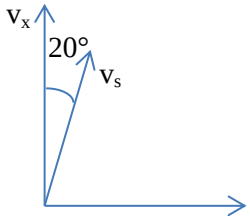

If v_x is known, v_s can be calculated through the relation below.

$$\cos(20°) = \frac{v_s}{v_x} \Rightarrow v_s = \cos(20°) * v_x$$

The pipe diameter is 0.104 m which gives a circumference of 0.3267 m. The rotational speed of the flow in rpm corresponding to the velocity v_s can be calculated by following equation.

$$rpm = \frac{v_s}{0.3267} * 60$$

For an operating point with an exhaust mass flow rate of 0.26 kg /s and a mean density in the inlet of 0.5937 kg/m^3 the velocity in the flow direction becomes

$$v_x = \frac{0.26}{0.5937} * \frac{1}{\left(\frac{0.104}{2}\right)^2 * \pi} = 51.55\ m/s$$

This will give a v_s of

$$v_s = \cos(20°) * v_x = 0.93969262 * 51.55 = 48.44\ m/s$$

and finally the rpm is calculated.

$$rpm = \frac{v_s}{O} * 60 = \frac{48.44}{0.104 * \pi} * 60 = 148.27 * 60 = 8896$$

B Appendix – Calculation of droplet evaporation, Stoke's number and thermal response time

Droplet evaporation time and length

The D^2-law presented in (*) was used to calculate an approximation of the evaporation time. The maximum and minimum size of the injected droplets is 300 μm and 2 μm respectively.

$$D_0^2 + D^2 = \lambda t \qquad (*)$$

To calculate the evaporation time, the evaporation rate coefficient λ is needed and the experimental data from [32] was used to calculate this. Three data points at 673 K were taken from Figure 14 in [32] and these are listed in Table 7.

Table 7: Experimental data from [32].

Initial diameter (D_0) of Urea-Water-Solution Droplet [mm]	Rate Coefficient (λ) [mm^2/s]
0.07	0.036
1	0.039
1.34	0.044

A linear regression was constructed from these three points and is given in equation (**).

$$\lambda = 0.00565 * D_0 + 0.03513 \qquad (**)$$

By using these two equations and defining D=0, an approximate evaporation time for the largest and the smallest droplets could be calculated. The average velocity in the domain is 30 m/s (for a temperature of 658 K) and from this the typical length needed for evaporating the droplets can be calculated. The results are presented in Table 8.

Table 8: Calculated values of the evaporation time for the largest and the smallest simulated droplets.

Initial diameter (D_0) [μm]	Evaporation time (t) [s]	Needed length [m]
300	2.45	73.5
2	$1.14*10^{-4}$	0.00342

Hence, the evaporation time spans from less than ms up to a few seconds which emphasize the significance of the droplet size and residence time. It can be concluded that the largest droplets will not have enough time for evaporation since these will need approximately 70 m. This means that it is not possible to reach full conversion of urea if the droplet size is not reduced and there will be urea left that enters the SCR catalyst.

Stoke's number

To get an idea of how well the droplet will follow the flow and adjust to changes in the flow the Stoke's number was calculated for the largest and the smallest simulated droplets. The derived equations in this section comes from [19]. The Stoke´s number for a droplet is defined as

$$St = \frac{\tau_d}{\tau_f}$$

where τ_d is droplet response time and τ_f is the characteristic time scale for the flow. The droplet response time for non-Stoke's flow may be calculated by

$$\tau_d = \frac{\rho_d D_p^2}{18\mu_c} * \frac{C_D Re_p}{24}$$

where C_D is the drag coefficient that may be determined from the correlation below.

$$C_D = \frac{24}{Re_p}(1 + 0.15 Re_p^{0.687})$$

The material data used in the calculations are taken from [33] and the simulations and are displayed in Table 9.

Table 9: Material data used in the calculations.

Droplet density (ρ_d)	1104 kg/m^3
Density of the continuous phase (ρ_c)	0.6 kg/m^3
Dynamic viscosity of the continuous phase (μ_c)	1.716*10^{-5} Pa*s

The Reynolds number for the droplets is defined below. The relative velocity between the continuous and the dispersed ($|v_r|$) phase is needed.

$$Re_p = \frac{\rho_c |v_r| D_p}{\mu_c}$$

The initial spray velocity is 18 m/s but the spray is injected with an angle that differs 50° from a straight inlet (see Figure 21). This means that the spray velocity in the flow direction can be calculated as

$$u = \sin(50) * 18 = 13.8\, m/s$$

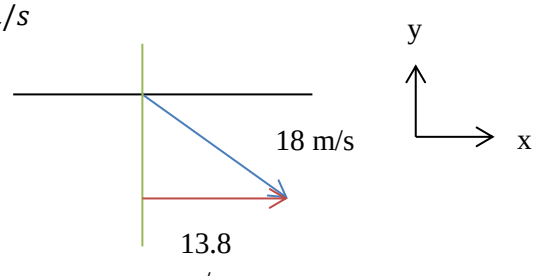

Figure 21: The black line represents the pipe wall and the green line is the normal to the wall. Since the spray is injected with an angle that differs 50° from the normal the velocity in the x-direction has to be calculated and is displayed with a red arrow.

The velocity of the continuous phase i.e. the exhaust gas flow is 55 m/s and the relative velocity then becomes 41.2 m/s. The time scale for the flow in this case is calculated as the characteristic time scale for the turbulence which is defined as

$$\tau_{turb} = \frac{k}{\varepsilon}$$

where k is the turbulent kinetic energy and ε is the dissipation of the flow. These values were extracted from the simulations and the result is presented below.

k	25.7 J/kg
ε	1.40*10^4 m^2/s^3
τ_{turb}	4.59*10^{-5} s

For a droplet diameter of 300 μm the Stoke's number was calculated to approximately 1800 i.e. St>>1. This means that the largest droplets do not follow the flow initially. For a droplet diameter of 2 μm the Stoke's number was calculated to approximately 0,1 i.e. St≈1. The smallest droplets will follow the flow to some extent from the moment they are injected. Hence, the flow field is an important factor for the spreading of the droplets and it should be preferable to have a turbulent flow that can allocate the droplets.

Thermal response time

The thermal response time is the time it takes for a droplet to respond to a change in temperature of the continuous phase. If it is assumed that temperature is uniform throughout the droplet and that radioactive effect is negligible, the equation for the particle temperature can be defined as

$$\frac{dT_d}{dt} = \frac{Nu_p}{2}\frac{12k_c}{\rho_p c_d D_p^2}(T_c - T_d)$$

where c_d is the specific heat of the droplet material and k_c is the thermal conductivity of the continuous phase. The temperatures T_c and T_d is the temperature of the continuous phase and the droplet respectively [34]. The Nusselt number for the droplets can be calculated from the correlation below

$$Nu_p = 2(1 + 0.3Re_p^{1/2}Pr^{1/3})$$

The Prandtl number is defined as

$$Pr = \frac{c_p \mu_c}{k_c}$$

where c_p is the specific heat of the continuous phase [20]. The thermal equation including the thermal response time (τ_T) for the particle can be written as [34]

$$\frac{dT_d}{dt} = \frac{1}{\tau_T}(T_c - T_d)$$

Hence, the thermal response time for the droplet may be calculated through following equation.

$$\tau_T = \frac{\rho_p c_d D_p^2}{12k_c(1+0.3Re_p^{1/2}Pr^{1/3})}$$

The droplet material is a urea-water solution consisting of urea (32.5wt %) and water (67.5wt %) and has an initial temperature of 30°. However, it is assumed to have the same material properties as water in these calculations. The continuous phase is simulated as air and the temperature varies with the power output from the engine. In these calculations it is assumed that the exhaust gases have a temperature of 400°. The material data that is used in the calculations was taken from [33] and the simulations and are displayed in Table 10.

Table 10: Material data used in the calculations.

Droplet density (ρ_p at 30°)	995.7 kg/m^3
Specific heat of the droplets (c_d at 30°)	4175 J/kg*K
Specific heat of the continuous phase (c_p at 400°)	1070 J/kg*K
Thermal conductivity of the continuous phase (k_c at 400°)	0.0515 W/m*K
Dynamic viscosity of the continuous phase	1.716*10^{-5} Pa*s

For a droplet diameter of 300 μm the τ_T was calculated to approximately 0.1 s and for a droplet diameter of 2 μm it was calculated to approximately $2*10^{-5}$ s.

C Appendix – Residence time and mixer pressure drop

Table 11: The mean residence time for a droplet from the injection point to the SCR inlet for all studied cases.

Configuration	Residence time [s]
No mixer	0.002
100mm	0.025
100,150mm	0.026
50,100,150mm	0.041
50,100mm	0.031
bef&aft inj	0.030
100,150mm mirror	0.010
100,150mm mid inj	0.010
100,150mm two inj	0.013

Table 12: Pressure drop over the mixer(s) for all studied configurations.

Configuration	Pressure drop [Pa]
100mm	1700
100,150mm	2600
50,100mm	2600
50,100,150mm	3700
bef&aft flex	3200
bef&aft inj	2900
100,150mm mirror	3700